Received: 17 April 2024 | Revised: 9 September 2024 | Accepted: 12 September 2024

DOI: 10.1111/bph.17366

RESEARCH ARTICLE

The endocannabinoid anandamide mediates anti-inflammatory effects through activation of NR4A nuclear receptors

Tom Teichmann[1,2] | Beatrice Pflüger-Müller[1,2] | Virna Margarita Martín Giménez[3] | Fiona Sailer[4] | Henrik Dirks[1,2] | Simonida Zehr[1,2] | Timothy Warwick[1,2] | Felix Brettner[5] | Paola Munoz-Tello[6] | Andreas Zimmer[7] | Irmgard Tegeder[8] | Dominique Thomas[8,9] | Robert Gurke[8,9] | Stefan Günther[10] | Jan Heering[9] | Ewgenij Proschak[9,11] | Gerd Geisslinger[8] | Iris-S. Bibli[2,12] | Dagmar Meyer zu Heringdorf[13] | Walter Manucha[14,15] | Maike Windbergs[5] | Stefan Knapp[11,16] | Andreas Weigert[4] | Matthias S. Leisegang[1,2] | Douglas Kojetin[6,17] | Ralf P. Brandes[1,2]

[1]Goethe University Frankfurt, Institute for Cardiovascular Physiology, Frankfurt, Germany

[2]German Centre of Cardiovascular Research (DZHK), Frankfurt, Germany

[3]Instituto de Investigaciones en Ciencias Químicas, Facultad de Ciencias Químicas y Tecnológicas, Universidad Católica de Cuyo, San Juan, Argentina

[4]Institute of Biochemistry I, Faculty of Medicine, Goethe University Frankfurt, Frankfurt, Germany

[5]Institute of Pharmaceutical Technology, Goethe University Frankfurt, Frankfurt am Main, Germany

[6]Department of Biochemistry, Vanderbilt University, Nashville, Tennessee, USA

[7]Institute of Molecular Psychiatry, Medical Faculty, University of Bonn, Bonn, Germany

[8]Institute of Clinical Pharmacology, Medical Faculty, Goethe-University Frankfurt, Frankfurt, Germany

[9]Fraunhofer Institute for Translational Medicine and Pharmacology ITMP and Fraunhofer Cluster of Excellence for Immune Mediated Diseases CIMD, Frankfurt, Germany

[10]Max-Plank-Institute for Heart and Lung Research (MPI-HLR), Bad Nauheim, Germany

[11]Institute of Pharmaceutical Chemistry, Goethe University Frankfurt, Frankfurt, Germany

[12]Institute for Vascular Signaling, Centre for Molecular Medicine, Goethe University Frankfurt, Frankfurt am Main, Germany

[13]Institute of General Pharmacology and Toxicology, University Hospital Frankfurt, Goethe University Frankfurt, Frankfurt, Germany

[14]Instituto de Medicina y Biología Experimental de Cuyo (IMBECU), Consejo Nacional de Investigaciones Científicas y Tecnológicas (CONICET), Mendoza, Argentina

[15]Departamento de Patología, Área de Farmacología, Facultad de Ciencias Médicas, Universidad Nacional de Cuyo, Mendoza, Argentina

[16]Structural Genomics Consortium (SGC), Buchmann Institute for Life Sciences, Goethe University Frankfurt, Frankfurt am Main, Germany

[17]Center for Structural Biology and Institute for Chemical Biology, Vanderbilt University, Nashville, Tennessee, USA

Correspondence
Ralf P. Brandes, Institut für Kardiovaskuläre Physiologie, Fachbereich Medizin der Goethe Universität, Theodor-Stern-Kai 7, Frankfurt am Main 60590, Germany.
Email: brandes@vrc.uni-frankfurt.de

Background and purpose: Endocannabinoids are lipid mediators, which elicit complex biological effects that extend beyond the central nervous system. Tissue concentrations of endocannabinoids increase in atherosclerosis, and for the endocannabinoid

Abbreviations: AEA, anandamide, N-arachidonoyl-ethanolamine; AF1, activation function 1; 2-AG, 2-arachidonoylglycerol; C-DIM12, 4-Chlorophenyl-3,3′-diindolylmethane; CsnB, Cytosporone B; CYP/P450, Cytochrome P450; DBD, DNA binding domain; EBM, endothelial basal medium; FAAH, fatty acid amide hydrolase; FCS, fetal calf serum; HAoSMC, Human aortic smooth muscle cells; LBD, Ligand binding domain; MCDB, Molecular, Cellular and Developmental Biology 131; PPAR, peroxisome proliferator-activated receptor; PUFA, polyunsaturated fatty acid; SMC, smooth muscle cell.

Funding information
This study was supported by the US National Institutes of Health (NIH) Grant R01AG070719 from the National Institute on Aging (DJK); the Leistungszentrum Innovative Therapeutics (TheraNova) funded by the Fraunhofer Society and the Hessian Ministry of Science and Arts and Deutsche Forschungsgemeinschaft (DFG) projects: GRK2336 (AVE), Projektnummer 321115009; SFB1039 Projektnummer 204083920; SFB1531 Projektnummer 456687919; Cardio-Pulmonary Institute (CPI) (EXC2026 Projektnummer 390649896); the Goethe-University Frankfurt and the DZHK (Deutsches Zentrum für Herz-Kreislauf-Erkrankungen) and the Dr. Rolf Schwiete-Stiftung. This study was also supported by the Agencia Nacional de Promoción Científica y Tecnológica with PICT 2020 Serie A 4000 and was also funded by a stipend of the German Academic Exchange Service (DAAD).

N-arachidonoyl-ethanolamine (anandamide, AEA), this has been linked to an anti-inflammatory function. In this study, we set out to determine the anti-inflammatory mechanism of action of AEA, specifically focusing on vascular smooth muscle cells.

Experimental approach: RNA-sequencing, RT-qPCR, LC-MS/MS, NanoBit, ChIP, microscale thermophoresis, NMR structural footprinting, Gal4 reporter gene assays and loss of function approaches in cell and ex vivo organ culture were used.

Key results: AEA pretreatment attenuated the cytokine-mediated induction of inflammatory gene expression such as CCL2. This effect was also observed in preparations obtained from cannabinoid receptor knockout mice and after pertussis toxin treatment. The anti-inflammatory effect of AEA required preincubation, suggesting an effect through gene induction. AEA increased the expression of the nuclear receptors NR4A1 and NR4A2. Knockdown and knockout of these receptors blocked the AEA-mediated anti-inflammatory effect in cell culture and aortic organ culture, respectively. Conversely, NR4A agonists (CsnB, C-DIM12) attenuated inflammatory gene expression. AEA binds to NR4A, and mutations in NR4A attenuated this effect. The interaction of AEA with NR4A caused recruitment of the nuclear corepressor NCoR1 to the CCL2 promoter, resulting in gene suppression.

Conclusion and implications: By binding to NR4A, AEA elicits an anti-inflammatory response in vascular smooth muscle cells. NR4A-binding by AEA analogues may represent novel anti-inflammatory agents.

KEYWORDS
AEA, endocannabinoids, NR4A

1 | INTRODUCTION

Endocannabinoids are neurotransmitters linked to the control of appetite, reward, memory and pain (Lu & Mackie, 2016). The best characterized endocannabinoids are **N-arachidonoyl-ethanolamine** (anandamide, AEA) and **2-arachidonoylglycerol** (2-AG) (Battista et al., 2012). Despite their structural similarities, both lipids have distinct synthesis and degradation pathways. Unlike classical neurotransmitters that are stored in vesicles and released in response to an action potential, endocannabinoids are synthesized de novo on demand or released from membrane lipids upon increased intracellular calcium concentration or activation of protein kinase C (Pandey et al., 2009).

The biological action of endocannabinoids is terminated by enzymatic degradation. AEA, for instance, is rapidly metabolized by several enzymes: **fatty acid amide hydrolase** (FAAH), **cyclooxygenase 2** (COX2), lipoxygenases (LOX) and cytochrome P450 (CYP). Depending on enzyme expression, this leads to tissue-selective accumulation and degradation of the lipid, which provides one explanation for the tissue-selective effects of AEA (Maccarrone, 2017; Piscitelli & di Marzo, 2012). Indeed, while the biological effects of AEA in the central nervous system are well documented, the somatic effects of this endocannabinoid are controversial. A cardioprotective and vasodilator function of AEA have been demonstrated in some studies, but the underlying mechanisms remain unclear. (Baranowska-Kuczko et al., 2014; Ellis et al., 1995; Stanley et al., 2016; Tuma & Steffens, 2012).

What is already known?

- Endocannabinoids, such as anandamide (AEA), are signalling lipids that impact appetite, reward, inflammation and pain.
- In atherosclerosis, endocannabinoid levels increase, with AEA being specifically associated with anti-inflammatory effects.

What does this study add?

- In vascular smooth muscle cells (VSMCs), AEA exerts anti-inflammatory effects independent of classical endocannabinoid receptors.
- AEA induces and activates NR4A1 and NR4A2, thereby mediating its anti-inflammatory effects in VSMCs.

What is the clinical significance?

- NR4A agonists, like AEA, have the potential to serve as new anti-inflammatory agents.

AEA and other endocannabinoids mediate their neurological effects primarily through the G_i-coupled cannabinoid receptors **CB_1** and **CB_2** receptors (Munro et al., 1993). Whereas CB_1 is more abundant in the central nervous system, CB_2 is preferentially expressed in cells of the immune system (Battista et al., 2012). When presented at higher concentrations, endocannabinoid signalling under certain conditions has also been attributed to the activation of alternative receptors such as the **transient receptor potential vanilloid type-1** (TRPV1) and **transient receptor potential ankyrin type-1** (TRPA1) channels as well as the G-protein coupled receptors **GPR55** and **GPR119** (Ligresti et al., 2016; Maccarrone, 2017; Pertwee et al., 2010; Zygmunt et al., 1999). Also, classic lipid receptors like the peroxisome proliferator-activated receptor (PPARs) family of nuclear receptors can mediate endocannabinoid effects (O'Sullivan, 2007). However, the latter effect requires efficient cellular uptake and thus particularly high extracellular concentrations.

In the present study, we followed up on our previous observation of an AEA-mediated anti-inflammatory effect in human aortic smooth muscle cells (HAoSMCs) (Pflüger-Müller et al., 2020). We sought to identify the underlying mechanism and signalling pathway to determine whether AEA could be a potential anti-inflammatory treatment. Our investigation revealed that the anti-inflammatory effects of AEA are mediated by the activation of members of the nuclear receptor subfamily 4A (NR4A), namely, **NR4A1** and **NR4A2**, which can also be exploited pharmacologically.

2 | METHODS

2.1 | Cell culture

Human aortic smooth muscle cells (HAoSMC) were obtained from PELOBiotech (#354-05a, Planegg, Germany). The cells were cultured on collagen-coated dishes in Smooth Muscle Cell Medium (PELOBiotech, #PB-MH-200-2190, Germany) with 8% heat-inactivated fetal calf serum (FCS), L-glutamine, penicillin (50 U ml^{-1}) and streptomycin (50 µg ml^{-1}) (#15140-122, Gibco, New York, United States), EGF, bFGF and insulin (PELOBiotech, Germany) in a humidified atmosphere of 5% CO_2 at 37°C. Cells from passage 5 to 10 were used. For each experiment, at least three different batches of HAoSMC were used.

Human embryonic kidney 293 cells (HEK293) cells were obtained from ATCC (#CRL-11268, Manassas, United States) and cultured in Modified Eagle's Medium (MEM, Gibco) supplemented with 8% heat-inactivated FCS, non-essential amino acids (NEAA, 0.1 mM), sodium pyruvate (1 mM) and gentamycin (50 µg ml^{-1}) in a humidified atmosphere of 5% CO_2 at 37°C.

2.2 | Anandamide (AEA) treatment

HAoSMC and freshly isolated smooth muscle cells isolated from the aorta of CB_1 and CB_2 receptor knockout mice were exposed to media with L-glutamine and 1% FCS overnight or for at least 16 h. The next day, cells were incubated in media with 1% FCS, L-glutamine and 10 µM diclofenac (Sigma Aldrich, #D-6899, Taufkirchen, Germany) for 1 h and treated with 10 µM AEA (Sigma-Aldrich) or EtOH as solvent control (CTL) for 2.5 h. Diclofenac was used to prevent cyclooxygenase-mediated breakdown of AEA. Subsequently, 10 ng ml^{-1} IL1β was added for 1.5 h. Treatment of HEK293 cells was similar to that of HAoSMC. Next to AEA, the following compounds were used (see Table 1).

Murine aortic rings were cultured in endothelial basal medium (EBM) with 0.1% bovine serum albumin (BSA) and 10 µM diclofenac. Treatment was performed in the presence of 10 µM diclofenac and pre-treatment with 10 µM AEA overnight. The next day, murine IL1β (10 ng ml^{-1}) was added and incubated for 1.5 h.

TABLE 1 Compounds with abbreviations used, and concentrations.

Compound	Abbreviation	Concentration	Company
2-arachidonoylglycerol	2-AG	10 µM	Tocris
4-Chlorophenyl-3,3′-diindolylmethane	CDIM-12	15 µM	Sigma-Aldrich
Arachidonoyl amide	AAA	10 µM	Sigma-Aldrich
Arachidonoyl-2′-Fluoroethylamide	2FAEA	10 µM	Sigma-Aldrich
Arachidonoyl-ethanolamide phosphate	pAEA	10 µM	Sigma-Aldrich
Cytosporone B	CsnB	15 µM	Sigma-Aldrich
Docosahexaenoyl ethanolamide	DHEA	10 µM	Sigma-Aldrich
Docosatetraenoyl ethanolamide	DTEA	10 µM	Sigma-Aldrich
Eicosapentaeonyl ethanolamide	EPEA	10 µM	Sigma-Aldrich
Linoleoyl ethanolamide	LEA	10 µM	Sigma-Aldrich
N-arachidonoyl dopamine	NADA	10 µM	Sigma-Aldrich
Oleoylethanolamide	OEA	10 µM	Tocris
Palmitoylethanolamide	PEA	10 µM	Tocris
Prostaglandin A_1	PGA1	15 µM	Cayman
R(+) Methanandamide	MAEA	10 µM	Sigma-Aldrich

2.3 | Animals

Global knockout mice of Nur77 (NR4A1$^{-/-}$) and Nur1 (NR4A2$^{-/-}$) as well as double knockout of Nur77 and Nur1 (NR4A1/2$^{-/-}$) were generated using the Cre/loxP system by crossing Nur77$^{flox/flox}$ (obtained from the Jackson Laboratory, Maine, USA) and Nur1-$^{flox/flox}$ mice (kindly provided by Pierre Chambon; Sekiya et al., 2011) respectively, with CMV-GT-Rosa-CreERT2$^{TG/0}$. All knockout animals were generated on the C57BL/6 background. Global NR4A1 and/or NR4A2 deletion was induced by application of tamoxifen with the chow (400 mg kg^{-1}) for 10 days. Subsequently, tamoxifen free chow as 'wash out' period of 14 days was given. In the present study, control animals are defined as littermates, which did not receive tamoxifen treatment with the chow. Male CNR1$^{-/-}$ knockout mice were kindly provided by Prof. Dr. Andreas Zimmer, Institute of Molecular Psychiatry, University Bonn (Zimmer et al., 1999). The CB_1 gene was mutated in MPI2 embryonic stem cells. Homozygous animals were generated by back-crossing of chimeric and heterozygous C57/BL6J animals. Female CNR2$^{-/-}$ knockout mice were kindly provided by Prof. Dr. Irmgard Tegeder, Institute for Clinical Pharmacology, University Frankfurt am Main. All animals had free access to chow and water in a specified pathogen-free facility with a 12 h light/dark cycle, and all animal experiments were performed in accordance with the German animal protection law and were carried out after approval by the local authorities (Regierungspräsidium Darmstadt, Approval Number FU1268). Animal studies are reported in compliance with the ARRIVE guidelines (Percie du Sert et al., 2020) and with the recommendations made by the *British Journal of Pharmacology* (Lilley et al., 2020). Every mouse received an identification number for each experiment, and the experimenter was blinded for the genotype. Animal group sizes differ due to number of available littermates.

2.4 | Isolation and culture of murine aortic rings as well as smooth muscle cells

Mice (three animals per preparation) were killed with isoflurane overdose followed by perfusion with phosphate buffered saline (PBS). Aortae were removed and cleaned of adhering connective tissue. Subsequently, the aorta was cut into 1 mm rings and cultured for 16 h in endothelial basal medium (EBM) with 0.1% BSA and 10 µM diclofenac. Treatment was performed as described in the section 'AEA treatment'. Aortic rings were shredded using a tissue lyser for 5 min, followed by RNA isolation and RT-qPCR.

For cell isolation, vessels were cut open, the endothelium was scraped off and the tissue was extensively washed. Subsequently, the aortae were minced in 50 µl sterile Molecular, Cellular and Developmental Biology 131 (MCDB) medium with 0.1% BSA into 1 mm small pieces and subjected to collagenase dissociation (380 U ml^{-1}) for 60 min at 37°C with titration every 10 min. The supernatant of this procedure was pelleted and cultured in smooth muscle cell (SMC) basal medium from PELOBiotech (#PB-MH-200-2190) with 8% fetal calf serum (FCS) and insulin in fibronectin coated dishes.

2.5 | siRNA transfection

HAoSMC were seeded for 50% confluence and transfected the next day with Lipofectamine 3,000 in 8% FCS (without antibiotics) and 40 nM Stealth siRNA (Invitrogen, Darmstadt, Germany) for 48 or 72 h. Medium was changed after 24 h. Stealth RNAi™ siRNA Negative Control Lo GC (siScr1) was used as negative control. For knockdown of the respective gene, the following siRNAs were used: NR4A1 (#J-003426-08-0020, Invitrogen), NR4A2 (#J-003427-08-0020, Invitrogen), NR4A3 (#J-003428-07-0020, Invitrogen), PPARα (#4392421, Invitrogen) and PPARγ (#4390825, Invitrogen).

2.6 | LentiCRISPRv2

Guide RNAs (gRNA) targeting NR4A1, NR4A2 or NR4A3 were designed using the web-interfaces of CHOPCHOP (https://chopchop.rc.fas.harvard.edu/). The respective gRNAs (see Table 2) were cloned into a lentiCRISPRv2 vector backbone with BsmBI (Thermo Fisher, Karlsruhe, Germany) according to the standard protocol (Sanjana et al., 2014). After cloning, the gRNA containing LentiCRISPRv2 vectors were purified and sequenced. lentiCRISPRv2 was a gift from Feng Zhang (Addgene plasmid #52961; http://n2t.net/addgene:52961; RRID:Addgene_52961, Addgene, Watertown, USA) (Sanjana et al., 2014). Lentivirus was produced in Lenti-X 293 T cells (#632180, Takara) using polyethylenamine (#408727, Sigma-Aldrich), psPAX2 and pVSVG (pMD2.G). psPAX2 and pMD2.G were a gift from Didier Trono (Addgene plasmid #12260; Addgene plasmid #12259). LentiCRISPRv2-produced virus was transduced in HAoSMCs with polybrene transfection reagent (MerckMillipore, # TR-1003-G), and selection was performed with puromycin (0.5–0.7 µg ml^{-1}) for 8 days prior to RNA and genomic DNA isolation.

2.7 | Quantitative RT-qPCR

HAoSMCs were grown to confluence and treated as indicated. For RNA isolation, the RNA Mini Kit (Bio&SELL, Nürnberg, Germany) was used according to the manufacturer's instructions. For reverse transcription, RNA (500 ng) was mixed with oligo dT primers (Sigma-Aldrich, #O4387) and random hexamer (Sigma-Aldrich, #O4387) and subsequently reverse transcribed into cDNA using the SuperScript III reverse transcriptase (Thermo Fisher) according to the manufacturer's protocol. Quantitative RT-qPCR was performed in an AriaMX Cycler (Agilent) with SYBR Green Master Mix (BioRad) and analysed with the ΔΔCt method with ROX (BioRad) as a reference dye. GAPDH served as a housekeeping gene. The primers are indicated in Table 3. Data were analysed using the AriaMX qPCR software (Agilent).

TABLE 2 Sequence of the sgRNAs used for lentiviral CRISPR/Cas9.

gRNA No.	Sense sequence	Antisense sequence
NR4A1		
5′.1	CACCGCGGGGTCCCGGACTCGGTGC	AAACGCACCGAGTCCGGGACCCCGC
5′.2	CACCGTGGGACACCAGCACCGAGTC	AAACGACTCGGTGCTGGTGTCCCAC
5′.3	CACCGTGGTCACGGGGTCCCGGACT	AAACAGTCCGGGACCCCGTGACCAC
5′.4	CACCGGGGTCAGGGGGTCGCTTGCC	AAACGGCAAGCGACCCCCTGACCCC
3′.1	CACCGCCTTGAGGGCTCGGGGATAC	AAACGTATCCCCGAGCCCTCAAGGC
3′.2	CACCGAGAGAGCTATTCCATGCCTA	AAACTAGGCATGGAATAGCTCTCTC
3′.3	CACCGCTCCACACCTTGAGGGCTCG	AAACCGAGCCCTCAAGGTGTGGAGC
3′.4	CACCGATCCCCGAGCCCTCAAGGTG	AAACCACCTTGAGGGCTCGGGGATC
NR4A2		
5′.1	CACCGGGGCTTGTAGTAAACCGACC	AAACGGTCGGTTTACTACAAGCCCC
5′.2	CACCGGCTGTCCGGACAGGGGCATT	AAACAATGCCCCTGTCCGGACAGCC
5′.3	CACCGTTGTACCAAATGCCCCTGTC	AAACGACAGGGGCATTTGGTACAAC
5′.4	CACCGTGGAGGACTGCTGTCCGGAC	AAACGTCCGGACAGCAGTCCTCCAC
3′.1	CACCGATTCGCAAGCCCGCGTCCAT	AAACATGGACGCGGGCTTGCGAATC
3′.2	CACCGCATTCGCAAGCCCGCGTCCA	AAACTGGACGCGGGCTTGCGAATGC
3′.3	CACCGATGGACGCGGGCTTGCGAAT	AAACATTCGCAAGCCCGCGTCCATC
3′.4	CACCGGAGACGCGTGGCCGATCTGC	AAACGCAGATCGGCCACGCGTCTCC
NR4A3		
5′.1	CACCGGTATGTCTGCGCCGCATAAC	AAACGTTATGCGGCGCAGACATACC
5′.2	CACCGGCTATATTGGGCTTGGACGC	AAACGCGTCCAAGCCCAATATAGCC
5′.3	CACCGTGCGGCGCAGACATACAGCT	AAACAGCTGTATGTCTGCGCCGCAC
5′.4	CACCGCTATATTGGGCTTGGACGCA	AAACTGCGTCCAAGCCCAATATAGC
3′.1	CACCGTACGGCGTGCGAACCTGCGA	AAACTCGCAGGTTCGCACGCCGTAC
3′.2	CACCGCTACGGCGTGCGAACCTGCG	AAACCGCAGGTTCGCACGCCGTAGC
3′.3	CACCGAGGAGCTCGTCGTCTGGCGA	AAACTCGCCAGACGACGAGCTCCTC
3′.4	CACCGCAGGAGCTCGTCGTCTGGCG	AAACCGCCAGACGACGAGCTCCTGC

TABLE 3 Table of forward and reverse primers used in this study.

Primer name	Forward (5′-3′)	Reverse (3–5′)
Human CCL2	CAAGCAGAAGTGGGTTCAGGAT	TTAGCTGCAGATTCTTGGGTTGT
Murine CCL2	CCACTCACCTGCTGCTACTCATTC	GTCACTCCTACAGAAGTGCTTGAGG
Murine GAPDH	GTGTGAACGGATTTGGCCGTATTG	ACCAGTAGACTCCACGACATACTC
Human GAPDH	TGCACCACCAACTGCTTAGC	GGCATGGACTGTGGTCATGAG
Human NR4A1	CCCTGAAGTTGTTCCCCTCAC	GCCCTCAAGGTGTGGAGAAG
Human NR4A2	ACCACTCTTCGGGAGAATACA	GGCATTTGGTACAAGCAAGGT
Human NR4A3	CATACAGCTCGGAATACACCAC	CCCTCCACGAAGGTACTGATG

2.8 | RNA-sequencing

Total RNA was isolated with the RNA Mini Kit from Bio&Sell. On-column DNase digestion (DNase-Free DNase Set, Promega, Walldorf, Germany) was performed to remove any potential DNA contamination. Total RNA and library integrity were verified with LabChip Gx Touch 24 (Perkin Elmer, Rodgau, Germany). Following standard instructions, 500 ng- to 1 μg of total RNA was used as input for SMARTer Stranded Total RNA Sample Prep Kit–HI Mammalian (Clontech, Heidelberg, Germany). Sequencing was performed on a NextSeq500 instrument (Illumina, San Diego, USA) with v2 chemistry, resulting in average of 74 M reads per library with 1 × 75 bp single end setup. The resulting raw reads were assessed for quality, adapter content and duplication rates with FastQC (Andrews, 2010). Reaper Version 13-100 was employed to trim reads after a quality drop below a mean of Q20 in a window of 10 nucleotides (Davis et al., 2013). Only reads between 30 and 150 nucleotides were cleared for further analyses. Trimmed and filtered reads were aligned versus the Ensemble human genome version hg19 (GRCh37.p5) using STAR 2.4.0a with the parameter '--outFilterMismatchNoverLmax 0.1' to increase the maximum

ratio of mismatches to mapped length to 10% (Dobin et al., 2013). The number of reads aligning to genes was counted with featureCounts 1.4.5-p1 tool from the Subread package (Liao et al., 2014). Only reads mapping at least partially inside exons were admitted and aggregated per gene. Reads overlapping multiple genes or aligning to multiple regions were excluded. Differentially expressed genes were identified using DESeq2 version 1.62 (Love et al., 2014). Adjusted *p* values were determined by Benjamini-Hochberg correction with a *p* value of 0.05 considered significant. The Ensemble annotation was enriched with UniProt data (release 06.06.2014) based on Ensembl gene identifiers (Activities at the Universal Protein Resource [UniProt]).

2.9 | LC-MS/MS

Endocannabinoids and endocannabinoid-like substances were analysed by liquid chromatography-electrospray ionization-tandem mass spectrometry (LC-ESI-MS/MS) as described previously (Grill et al., 2019). Minor modifications were made due to the special requirements of tissue samples. In brief, tissue samples were homogenized in water/ethanol 3:1 (v/v) using a Qiagen tissue lyser, resulting in a tissue homogenate of 0.04 mg μl^{-1}. The analytes were extracted by liquid–liquid extraction with ethyl acetate/hexane 9:1 (v/v) using 200 µl tissue homogenate (8 mg tissue) after spiking with the respective isotopically labelled internal standards. Chromatographic separation of the analytes was done with an Agilent 1290 Infinity I UHPLC system equipped with an Acquity UPLC BEH C18 column (100 × 2.1 mm, 1.7 µm, Waters, Eschborn, Germany). The quantification of all analytes was carried out in a hybrid triple quadrupole-ion trap mass spectrometer QTRAP 6500+ (Sciex, Darmstadt, Germany) equipped with a Turbo-V-source operating in positive ESI mode. For all analytes, the concentrations of the calibration standards, quality controls and samples were evaluated by Analyst software 1.6.3 and MultiQuant software 3.0.2 (Sciex) using the internal standard method (isotope-dilution mass spectrometry). Calibration curves were calculated by linear regression with 1/x weighting.

2.10 | Nuclear magnetic resonance (NMR) structural footprinting

Recombinant ^{15}N-labelled Nurr1 LBD (NR4A2; residues 353 to 598) was expressed in *Escherichia coli* BL21(DE3) cells (Life Technologies, Darmstadt, Germany) using a pET-46 plasmid as a tobacco etch virus (TEV) protease-cleavable N-terminal hexahistidine tag fusion protein in M9 media supplemented with $^{15}NH_4Cl$ (Cambridge Isotope Labs, Inc., Tewksbury. USA). Nurr1 LBD was eluted against a 500 mM imidazole gradient through a Ni-NTA column, followed by overnight dialysis against a buffer without imidazole for TEV protease His tag cleavage at 4°C, loaded onto the Ni-NTA column to remove further contaminants and the tag, concentrated, then run through a S75 size exclusion column (GE healthcare, Frankfurt, Germany) in NMR buffer (20 mM KPO_4 pH 7.4, 50 mM KCl, and 0.5 mM EDTA).

Two-dimensional [^{1}H,^{15}N]-TROSY-HSQC NMR data were collected on a Bruker 700 MHz NMR spectrometer equipped with a QCI cryoprobe at 298 K using 200 µM ^{15}N-labelled Nurr1 LBD in NMR buffer containing 10% D_2O in the presence of 1 equivalent (200 µM) ligand or vehicle control (0.8% ethanol-d6). Data were processed using NMRFx (Norris et al., 2016) and analysed using NMRViewJ (Johnson, 2018). NMR chemical shift perturbation (CSP) and peak intensity analysis was performed by transfer of Nurr1 LBD NMR chemical shift assignments (Michiels et al., 2010) that we previously validated (de Vera et al., 2016, 2019; Munoz-Tello et al., 2020) from the vehicle to the 1X ligand spectra. CSPs were calculated using the minimal NMR chemical shift method (Williamson, 2013).

2.11 | NanoBit assay

NR4A1 and NR4A2 full length coding sequences were cloned into the NanoBit TK-Promoter construct pBit1.1 with N-terminal large Bit according to the manufacturers protocol (Promega, Madison, USA) using the restriction sites for SacI and EcoRI, and leaving out the Start-Met of the NR4A. NcoR1 with C-terminal small Bit was cloned based on the Myc-DDK-tagged construct in pCMV6 that was purchased from origene (cat#: RC213467). The sequence for Gly-Ser linker and NanoBit small Bit was amplified by PCR using pBit2.1-C as template (Promega #N197) and introduced in frame after the FLAG-tag. Positive control (FKBP:FRB; #N2016) and negative control (HaloTag with small Bit; #N202A) were provided by Promega NanoBit PPI System. HEK293 cells were transfected with 10 ng of each plasmid combination (Small BiT + Large BiT) with Lipofectamin 2000, and measurements were performed the next day in 100,000 cells in a Luminometer with the NanoGlo Live cell imaging substrate (Promega). After background recording (10 min), stimuli were added (AEA, PEA, OEA or 30 µM Rapamycin as positive control), and chemiluminescence was recorded for an additional 20 min.

2.12 | Chromatin immuno-precipitation (ChIP) in HAoSMC

HAoSMC were incubated in endothelial basal medium (EBM) without supplements and additional 1% FCS overnight. The next day, 10 µM diclofenac was added and incubated for 1 h. Afterwards, cells were treated with AEA for 2 and 1 h with 10 ng ml^{-1} IL1β. Cells were cross-linked with formaldehyde (1%, 10 min, Sigma Aldrich). To stop cross-linking, glycin (0.1 M, 5 min) was added. Cells were washed twice with cold PBS, scraped and transferred to Falcon tubes and centrifuged for 5 min at 800 ×*g* at RT. Nuclear isolation was performed with the truCHIP™ Chromatin Shearing Kit (Covaris, Woburn, United States) according to the manufacturers protocol. Afterwards, the lysates were sonicated with a Bioruptur Plus (10 cycles, 30 s on, 90 s off; Diagenode, Seraing, Belgium) at 4°C. Debris were removed by centrifugation, and the lysates were diluted 1:3 in dilution buffer (20 mmol L^{-1} Tris/HCl pH 7.4, 100 mmol L^{-1} NaCl, 2 mmol L^{-1} EDTA, 0.5% Triton

X-100 and protease inhibitors). After preclearing with 25 µl DiaMag protein A-coated magnetic beads (Diagenode) for 60 min at 4°C, samples were incubated overnight at 4°C with 3 µg of each antibody: anti-Nur77 (Santa Cruz Biotechnology Cat# sc-365113, RRID:AB_10709310), anti-Nurr1 (Santa Cruz Biotechnology Cat# sc-376984, RRID:AB_2893391). Five per cent of the samples served as input. The antibody complexes were collected with 50 µl DiaMag protein A-coated magnetic beads (Diagenode, Seraing, Belgium) for 3 h at 4°C, subsequently washed twice for 10 min with each of the wash buffers 1–3 (wash buffer 1: 20 mmol L^{-1} Tris/HCl pH 7.4, 150 mmol L^{-1} NaCl, 0.1% SDS, 2 mmol L^{-1} EDTA, 1% Triton X-100; wash buffer 2: 20 mmol L^{-1} Tris/HCl pH 7.4, 500 mmol L^{-1} NaCl, 2 mmol L^{-1} EDTA, 1% Triton X-100; wash buffer 3: 10 mmol L^{-1} Tris/HCl pH 7.4, 250 mmol L^{-1} lithium chloride, 1% Nonidet, 1% sodium deoxycholate, 1 mmol L^{-1} EDTA) and finally washed with TE-buffer pH 8.0. Elution of the beads was done with elution buffer (0.1 M $NaHCO_3$, 1% SDS) containing 1× proteinase K (Diagenode, Seraing, Belgium) and shaking at 600 rpm for 1 h at 55°C, 1 h at 62°C and 10 min at 95°C. Subsequently, the eluate was purified with the QiaQuick PCR purification kit (Qiagen, Hilden, Germany) and subjected to RT-qPCR analysis (see Table 4). Enriched NR4A1 and NR4A2 motifs were compared against the JASPAR^{2024} (Fornes et al., 2020) motif database.

2.13 | Microscale thermophoresis

Recombinant purified proteins of NR4A1 (#TP302202, Origene, Rockville, USA), A2 (TP321280, Origene) and A3 (# TP323629, Origene) were labelled at their cysteine sites with the Monolith NT protein labelling kit green-NHS (#MO-L002, NanoTemper Technologies, München, Germany). Serial dilutions of the potential ligands were generated in thermophoresis buffer. A fixed amount of labelled protein was added 1:1 to the ligand dilutions to a total volume of 20 µl (10 µl ligand or solvent control plus 10 µl protein). The mixtures were filled into capillaries (#MO-K025, NanoTemper Technologies) coated with specially designed polymer to prevent surface adsorption. The measurements were performed with a Monolith NT.015T Microscale Thermophoresis instrument (NanoTemper Technologies) at 20–80% laser intensity with blue light. Ligand effects were quantified using the NanoTemper software and the thermophoresis with jump mode. ΔF was quantified by $F_{CTL}-F_{ligand}$ for each concentration.

2.14 | Immunofluorescence staining

Cells were fixed by adding a final concentration of 2% paraformaldehyde in PBS for 10 min, followed by washing and 2% glycine for 10 min. Cells were permeabilized with 0.05% Triton X-100 for 10 min and blocked for 30 min with 3% BSA. The NR4A1 antibody (Thermo Fisher Scientific Cat# MA5-32647, RRID:AB_2809924) or NR4A2 antibody (Proteintech Cat# 10975-2-AP, RRID:AB_2153760) was incubated overnight at 4°C. The secondary antibody staining was performed the next day for 30 min incubation. In addition, DAPI was added for 10 min to counterstain nuclei. Images were acquired with a Zeiss LMS780 laser scanning microscope. Analysis of staining intensity was performed with ImageJ version 1.48 (Schindelin et al., 2012).

2.15 | Protein isolation and western blot analysis

For protein measurements, HAoSMCs were treated with AEA for 1 h and 10 ng ml^{-1} Interleukin-1 (IL1)-β (#200-01B, Peprotech) or 10 ng ml^{-1} tumour necrosis factor (TNF)-α (#300-245 01A, Peprotech) or Lipopolysaccharide (LPS) from *E. coli* (#L3024, Sigma) for 3 h. Subsequently, cells were washed twice with ice cold Hank's buffer and lysed with Triton X-100 lysis buffer (20 mM TRIS/Cl pH 391 7.5, 150 mM NaCl, 10 mM NaPi, 20 mM NaF, 1% Triton X-100, 2 mM orthovanadate (OV), 10 nM 392 okadaic acid, protein-inhibitor mix (PIM) and 40 µg ml^{-1} phenylmethylsulfonylfluorid). Cells were centrifuged for 10 min at 13.000 ×*g* at 4°C. Supernatant was collected, and protein concentration was determined by Bradford assay. Equal amounts of protein were boiled in sample buffer and separated by SDS-PAGE gel electrophoresis. The gels were blotted onto a nitrocellulose membrane and blocked in Rotiblock (Carl Roth, Germany). Infrared-fluorescent-dye-conjugated secondary antibodies were purchased from Licor (Bad Homburg, Germany) and detected with an infrared-based laser scanning detection system (Odyssey Classic, Licor, Bad Homburg, Germany). Antibodies were as follows: anti-CCL2 (Santa Cruz Biotechnology Cat# sc-52877, RRID:AB_628862) and anti-β-Actin (Cell Signalling Technology Cat# 4970, RRID:AB_2223172). The Immuno-related procedures used comply with the recommendations made by the *British Journal of Pharmacology* (Alexander et al., 2018).

TABLE 4 Table of ChIP primers used

Name	Forward (5′-3′)	Reverse (3–5′)
CCL2 TSS	TCCCTCCTCCTGCTTGACTC	AGTCTCAGCCTCTCGGTTCC
CCL2 −200 bp	GCTTCAGAGAAAGCAGAATC	TTCACTGCTGAGACCAAATG
CCL2 −600 bp	AGCAGGCTATTTAACCCTTC	GGCATAGACAGCATGTAGTG
CCL2 −1,000 bp	ATATTCCTGGCAGAGTAAGC	TCATAGAAGCCTAGCAGAAC
GAPDH	TGGTGTCAGGTTATGCTGGGCCAG	GTGGGATGGGAGGGTGCTGAACAC

2.16 | Gal4 reporter gene assay

For Gal4 reporter gene assays, plasmid mixtures of pGL4.35 luc2p/9x (#9PIE137, Promega) and one of the Gal4-fusion nuclear receptor plasmids pFA-CMV-hNur77-LBD, pFA-CMV-hNURR1-LBD and pFA-CMV-hNOR1-LBD coding ligand binding domain (LBD) of the canonical isoforms of the human nuclear receptors Nur77 (uniprot entry: hNUR77–P22736, residues 358–598), Nurr1 (uniprot entry: hNURR1–P43354, residues 359–598) and NOR1 (isoform alpha; uniprot entry: hNOR1–Q92570–1, residues 393–626) were used.

Overexpression of the respective plasmids was performed by electroporation with the Neon™ Transfection System (ThermoFisher) (1,000 V; 30 ms; 2 pulses). The pGL4.35 luc2p/9x plasmid on its own served as negative control. HAoSMCs were seeded on collagen-coated dishes. Twenty-four hours after electroporation, cells were treated as described in the section 'AEA treatment'. Subsequently, luciferase activity was measured by dual-luciferase reporter gene assay and luminescence measurement.

2.17 | Human samples

Carotid plaques material was obtained from patients who underwent carotid endarterectomy as outlined previously (Bibli et al., 2019). The present study followed the Code of Ethics of the World Medical Association (Declaration of Helsinki). The study protocol was approved by the Institutional Ethics Committee (Scientific and Ethic Committee of Hipokrateion University Hospital, PN1539), and all enrolled patients gave their informed consent. Samples were subjected to RT-qPCR as well as lipid measurements by LC-MS/MS. After exclusion of measurement for low quality, a total of 26 samples were included in the study.

2.18 | Statistical analysis

All experiments were independently performed at least three times as indicated by the number (*n*) in the respective figure legend. Statistical analysis was performed, only when the number of experiments was 5 or more, using Prism 10.1.2. ANOVA followed by Tukey's test or Mann–Whitney test was used to evaluate statistical significance. Post-hoc tests were run only if F achieved $P<0.05$ and there was no significant variance inhomogeneity.

A non-parametric Spearman correlation with a 95% confidence interval was used for human correlation statistics. Values of $P \leq 0.05$ were considered significant. All data are expressed as mean ± standard error of mean (SEM). Data and statistical analysis complied with the recommendations of the British Journal of Pharmacology on experimental design and analysis in pharmacology (Curtis et al., 2022).

2.19 | Nomenclature of targets and ligands

Key protein targets and ligands in this article are hyperlinked to corresponding entries in the IUPHAR/BPS Guide to PHARMACOLOGY http://www.guidetopharmacology.org and are permanently archived in the Concise Guide to PHARMACOLOGY 2023/23 (Alexander, Christopoulos et al., 2023; Alexander, Cidlowski et al., 2023; Alexander, Fabbro et al., 2023; Alexander, Mathie et al., 2023).

3 | RESULTS

3.1 | The anti-inflammatory effect of AEA is independent of classic cannabinoid receptors

To investigate the underlying mechanism behind the anti-inflammatory effects of AEA, we reproduced a previous experiment in which we demonstrated that preincubation with AEA attenuated IL1β-, TNFα and LPS mediated induction of **CCL2** (*MCP-1*) in human aortic smooth muscle cells (HAoSMC) (Pflüger-Müller et al., 2020) (Figures 1a and S1). Similar to this previous study, diclofenac was present in each subgroup of all experiments to prevent cyclooxygenase-dependent degradation of AEA (Elron-Gross et al., 2008). To determine whether this anti-inflammatory effect of AEA was a general feature of endocannabinoids, the response of palmitoylethanolamide (PEA), oleoylethanolamide (OEA) and 2-arachidonoyl glycerol (2-AG) was determined. Interestingly, only AEA, but not the other endocannabinoids, impaired the IL1β-induced CCL2 expression (Figure 1a,b), suggesting a CB-receptor independent mechanism. To specifically address this aspect, smooth muscle cells isolated from the aorta of CB_1 and CB_2 receptor knockout mice were analysed. Consistent with aortic SMCs of wild type (WT) mice, AEA suppressed cytokine-mediated CCL2-induction (Figure 1c). Moreover, pertussis toxin (PTX), which inhibits $G\alpha_i$-signalling (Mangmool & Kurose, 2011), also failed to block the response to AEA (Figure 1d). Collectively, these experiments suggest that classical CB receptors do not mediate the anti-inflammatory effect of AEA in vascular SMCs.

3.2 | The anti-inflammatory effects of anandamide (AEA) require a PUFA- and an ethanolamide group

To further characterize the structural requirements linked to the effect of AEA, different derivatives were studied. The anti-inflammatory activity was consistent among all compounds containing both a polyunsaturated fatty acid (PUFA) group and an acyl-amide moiety with ethanolamine derivatives. Conversely, compounds like PEA and OEA, lacking the PUFA group, or 2-AG and AAA, lacking the amide group, exhibited no activity (Figure 1e,f).

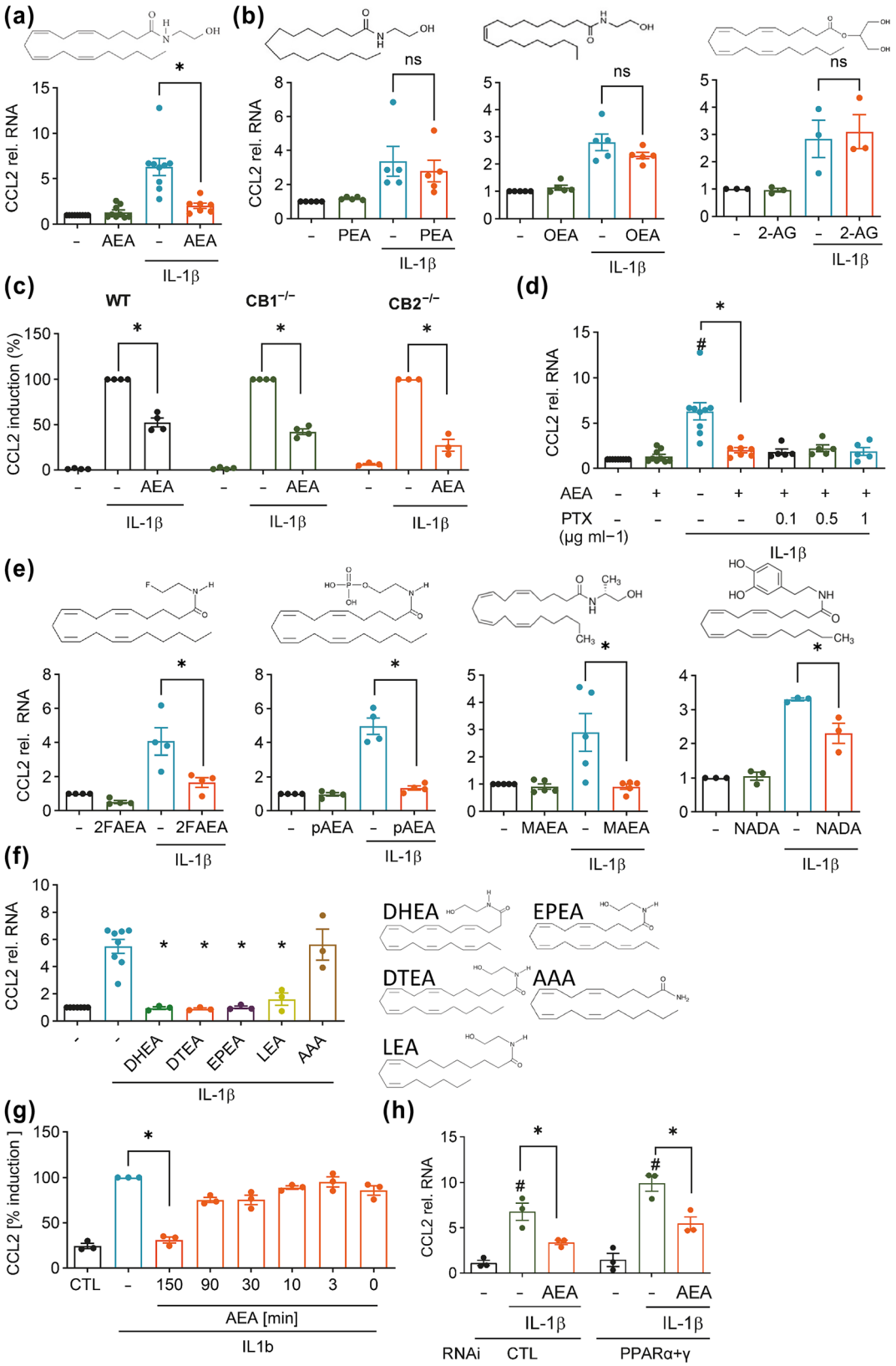

FIGURE 1 Legend on next page.

These results make it unlikely that AEA acts through other surface lipid receptors (i.e., **EP receptors** or similar). Also, as the effect required relatively high concentrations of AEA, it seems plausible that AEA is taken up by cells and acts on lipid-binding nuclear receptors. Indeed, blocking cellular uptake of AEA with AM404 (N-[4-hydroxyphenyl]arachidonylamide) (10 μM) (Beltramo et al., 1997) was able to prevent induction of some AEA responsive genes such as NEAT1 (Pflüger-Müller et al., 2020). AM404 itself, being a potent prostanoid and transient receptor potential vanilloid 1 ($TRPV_1$) ligand (Mallet et al., 2010), had a strong inhibitory effect on IL1β-dependent CCL2 induction, so that these data should be handle with caution (data not shown). Intracellular effects mediated by nuclear receptors are typically delayed, as they result from changes in gene expression (Olivares et al., 2015). Consequently, it was therefore tested whether the effect of AEA differs between pre-incubation and simultaneous addition with IL1β. Indeed, a time course experiment revealed that when AEA was administrated shortly before or simultaneously with IL1β, its anti-inflammatory effect was drastically reduced (Figure 1g), suggesting an effect through gene induction. Given that peroxisome proliferator-activated receptors can be activated by AEA (O'Sullivan, 2007), the role of **PPARα** and PPARγ was studied using siRNA-mediated knockdown (Figure S2a). Down-regulation of both receptors, however, failed to impact the AEA response (Figure 1h). Collectively, these observations suggest that the inhibitory effect of AEA on IL1β-induced gene expression is specific to this particular endocannabinoid and unlikely to be mediated by the previously reported endocannabinoid family receptors.

3.3 | Nuclear orphan receptor family NR4A expression is induced by anandamide (AEA)

Lowly expressed nuclear receptors are often self-induced upon ligand binding (Rodríguez-Calvo et al., 2017). Self-induction would also be consistent with the observed required pre-incubation to render effective receptor responses. To address this, nuclear receptor expression levels were extracted from RNA-seq data (Figure 2a) and subsequently confirmed by RT-qPCR (Figure 2b). This revealed that the expression of only a single group of nuclear receptors, the NR4A family, was indeed increased by AEA. Importantly, NR4A receptors are known to be auto-induced upon ligand binding and to modulate inflammatory responses (Pearen & Muscat, 2010; Pei et al., 2005; Zhao & Bruemmer, 2010). Within the NR4A group, AEA more strongly induced NR4A1 and NR4A2, whereas IL1β only had a minor effect on the expression of these receptors. In contrast, the cytokine evoked a strong induction of NR4A3, which was more pronounced than the response to AEA (Figure 2b). To establish the relationship between AEA and NR4A receptors also in patients, NR4A1, NR4A2 and NR4A3 mRNA levels were determined from carotid endarterectomy samples and correlated with AEA levels. Indeed, a positive significant correlation for NR4A2 was revealed (Figure 2c). Collectively, these findings support a connection between AEA and NR4A receptors.

3.4 | Anandamide (AEA) interacts with the nuclear orphan receptor family NR4A

If NR4A receptors mediated the anti-inflammatory effect of AEA, their pharmacological activators should elicit a similar response. Indeed, cytosporone B (CsnB), 4-Chlorophenyl-3,3′-diindolylmethane (CDIM-12) and prostaglandin A_1 (PGA1), which are known NR4A activators (Hammond et al., 2015; Rajan et al., 2020; Zhan et al., 2008), all prevented the IL1β-mediated CCL2 induction (Figure 3a). To provide support for a binding of AEA to NR4A receptors, microscale thermophoresis (Jerabek-Willemsen et al., 2014) was performed. As expected, the pharmacological agonists CsnB and CDIM-12 bound to NR4A1 and NR4A2 (Figure 3b). AEA also bound these receptors with similar potency. In contrast, NR4A3 was activated only by its known ligand prostaglandin A_2 (PGA2) (Kagaya et al., 2005) (Figure 3b). Although microscale thermophoresis is suitable to demonstrate interaction of the two compounds, we sought to confirm the interaction with NR4A1 or NR4A2 by a complementary technology. The best way to

FIGURE 1 Anti-inflammatory effects of AEA are independent of classical cannabinoid receptors. (a, b) CCL2 RT-qPCR of HAoSMC treated (a) anandamide (AEA, n = 9) and (b) palmitoylethanolamide (PEA, n = 5), oleylethanolamide (OEA, n = 5) or 2-arachidonoylglycerol (2-AG, n = 3) followed by treatment with IL1β. One-way ANOVA and Mann–Whitney test. Where n ≥ 5, $^*P < 0.05$. (c) CCL2 RT-qPCR of mAoSMC from WT, CB_1 or CB_2 KO mice treated with solvent (EtOH) or AEA with and without IL1β. $n = 4$. As n<5 for these experiments, statistical analysis was not carried out, and results should be regarded as preliminary. (d) CCL2 RT-qPCR of HAoSMC pretreated with PTX overnight, followed by treatment with solvent or AEA and IL1β. Ordinary one-way ANOVA and Mann–Whitney test. n = 5. Where n ≥ 5, $^*P < 0.05$ (-vs. treatment), $^{\#}P < 0.05$ (PTX + AEA vs. AEA). (e) CCL2 RT-qPCR of HAoSMC treated with solvent or arachidonoyl-2′-fluoroethylamide (2FAEA, n = 4), arachidonoyl ethanolamide phosphate (pAEA, n = 4), R(+) methananandamid (MAEA, n = 5) or N-arachidonoyldopamin (NADA, n = 4) and IL1β. One-way ANOVA. Where n ≥ 5, $^*P < 0.05$. (f) CCL2 RT-qPCR of HAoSMC treated with docosahexaenoyl ethanolamide (DHEA, n = 3), docosatetraenoyl ethanolamide (DTEA, n = 3), eicosapentaeonyl ethanolamide (EPEA, n = 3), linoleoyl ethanolamide (LEA, n = 3), arachidonoyl amide (AAA, n = 3) and IL1β (n = 8). One-way ANOVA and Mann–Whitney test and Mann-Whitney test. Where n ≥ 5, $^*P < 0.05$. (g) CCL2 RT-qPCR of HAoSMC. Different to the other experiments, AEA was administered at indicated timepoints followed by treatment with IL1β for 90 min. As n < 5, statistical analysis was not carried out and results should be regarded as preliminary. (h) CCL2 RT-qPCR of HAoSMC treated with solvent or AEA and IL1β after treatment with 40 nM siRNA against PPARα and PPARγ for 72 h. As n < 5, statistical analysis was not carried out and results should be regarded as preliminary. CTL, control; rel., relative to.

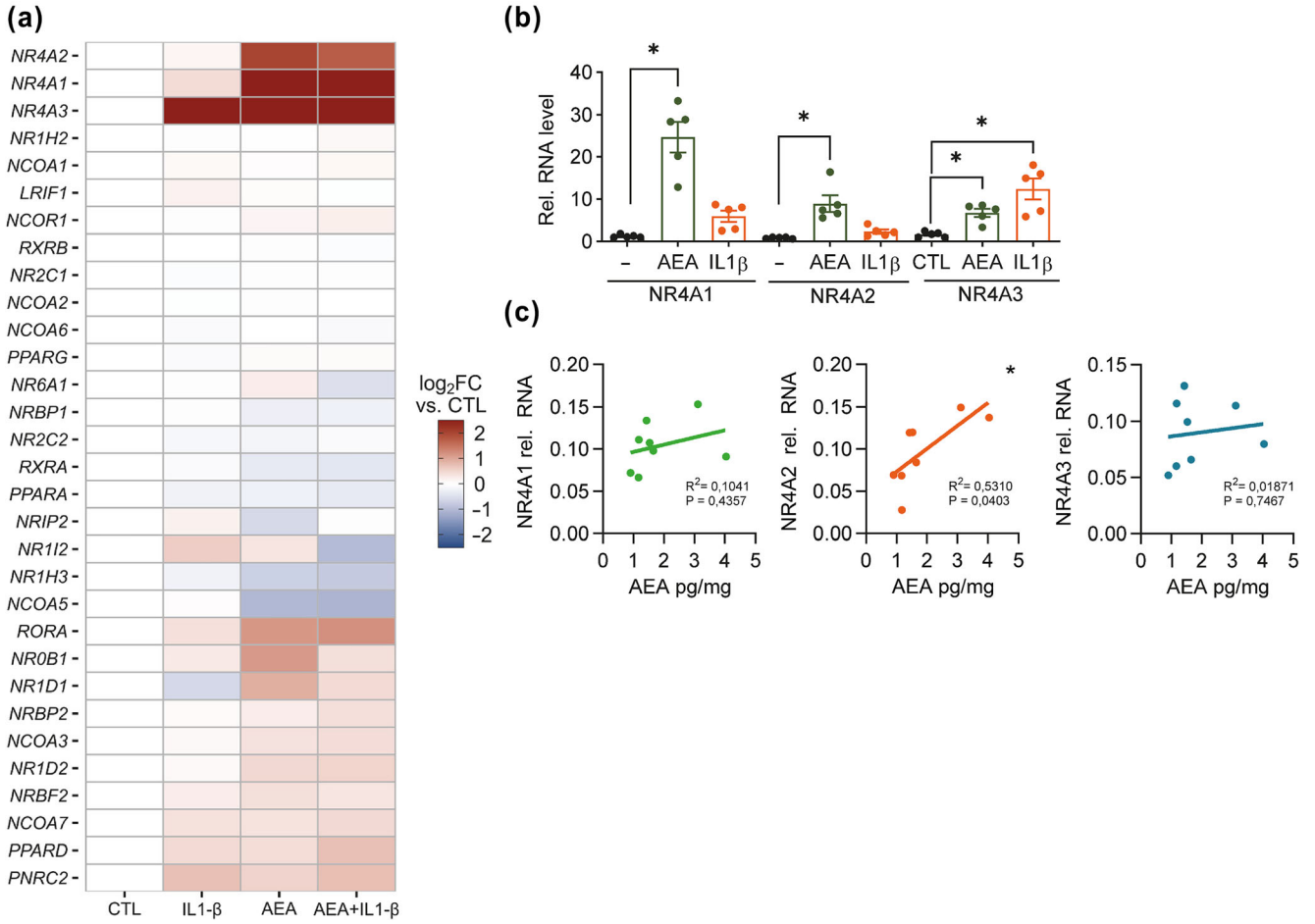

FIGURE 2 Nuclear orphan receptor family NR4A expression is induced upon AEA treatment. (a) Analysis of RNA sequencing data from HAoSMC after stimulation with solvent or AEA and IL1β. Change in nuclear receptor expression among different treatment conditions shown as $\log_2$FC vs. solvent (CTL). (b) RT-qPCR for the genes indicated of HAoSMC treated with solvent (CTL), AEA or IL1β for 4 h. n = 5 One-way ANOVA. *$P < 0.05$. (c) Correlation of endocannabinoid levels and NR4A expression in human carotids post-endarterectomy. A total number of 48 samples was used. To achieve a sufficient sensitivity, six samples were pooled prior to MS analysis, yielding a final number of n = 8 pool samples. Samples lacking LC-MS/MS data or lacking Ct values after RT-qPCR were excluded from the analysis. rel., relative to.

demonstrate ligand receptor interaction would be X-ray crystallography, as this technology also reveals the binding pocket of the ligand and details on ligand interaction with the receptor. Unfortunately, despite several attempts using AEA, phosphate-AEA and fluor-AEA in crystallization experiments with NR4A2, we obtained only apo-structures of this receptor possibly due to the limited solubility of these ligands or steric constrains of the receptor in the crystal environment (data not shown). We therefore used nuclear magnetic resonance (NMR) spectroscopy structural footprinting, which was previously successfully performed for the ligand binding domain (LBD) of NR4A2 (Munoz-Tello et al., 2020). Gratifyingly, NMR chemical shift perturbations (CSPs) and peak intensity changes resulting from the kinetics of ligand binding for ^{15}N-labelled NR4A2 LBD were observed in response to AEA treatment within helix 3, helix 6/7, helix 10/11 and helix 12, which confirms direct binding of AEA (Figure 3c–e). Moreover, AEA was previously shown to covalently bind to Cys566 (Figure 3e, green sticks). However, the NMR structural footprinting data indicate AEA binds to a different epitope, within the putative orthosteric ligand-binding pocket similar to (poly)unsaturated fatty acids (de Vera et al., 2019). As a second line of evidence for receptor activation, we established a Gal4 hybrid reporter gene assay (Paguio et al., 2010) for NR4A1 and NR4A2. In this assay, the LBD of the receptor is fused to the GAL4 DNA binding domain in one of the expression vectors. Cells are co-transfected with this and a second plasmid in which a firefly luciferase is under the control of multiple Gal4 upstream activator sequences, so that activation of the LBD results in luciferase induction. AEA increased luciferase expression for the NR4A1 (Figure S3) and NR4A2 (Figure 3f) construct to as similar extent as previously characterized agonists (Willems et al., 2020). Importantly, mutation of the amino acids Q568 and D408, which were identified by NMR to be affected by AEA, attenuated the GAL4-NR4A2 luciferase activity (Figure 3d,e). Collectively, these data demonstrated binding of AEA to NR4A1 and NR4A2.

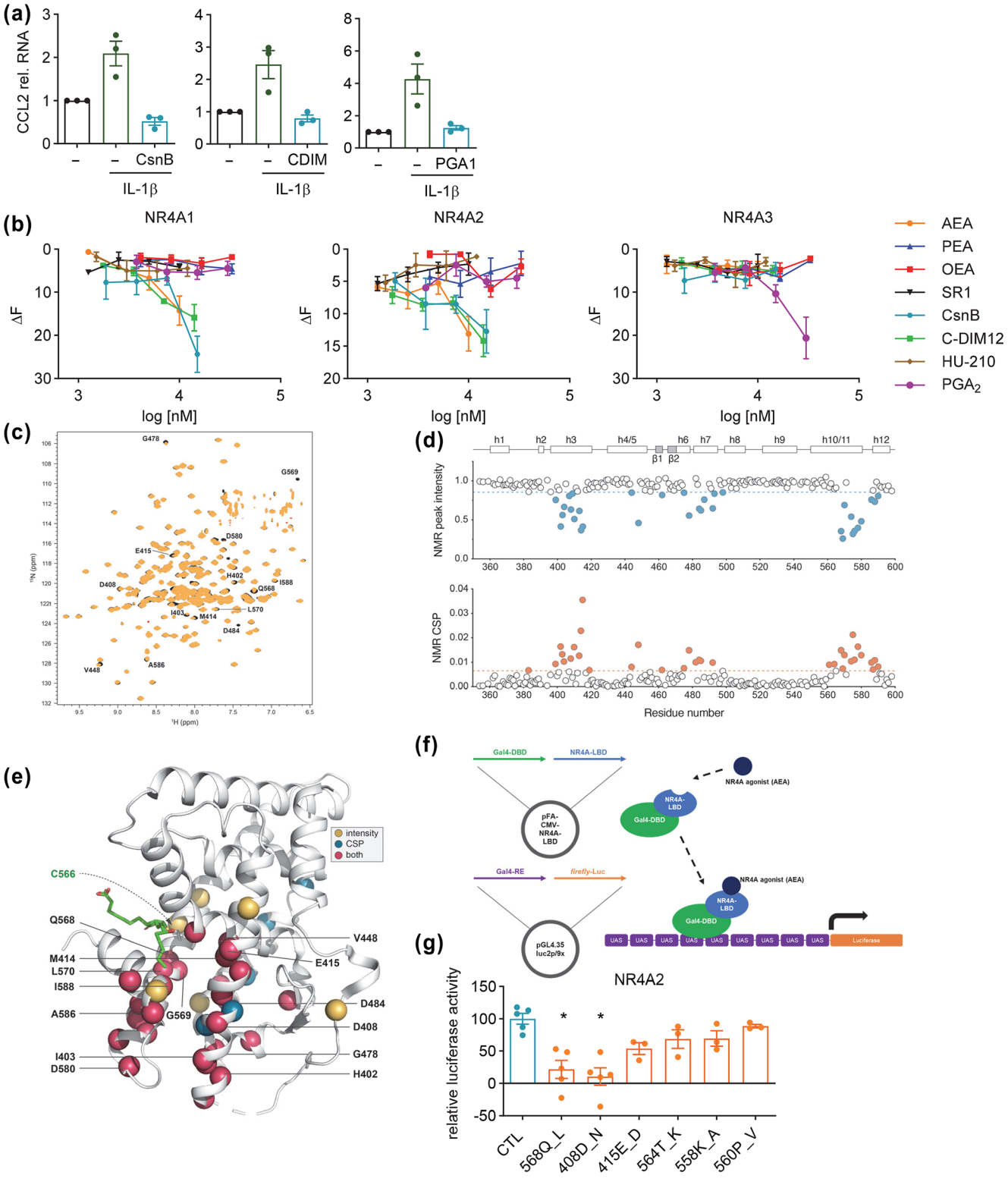

FIGURE 3 Legend on next page.

3.5 | Nuclear receptors NR4A1 and NR4A2 are recruited to the CCL2 gene locus upon anandamide (AEA) treatment

To study whether the inhibitory effect of AEA on IL1β-induced gene expression is directly mediated by NR4A receptors, we focused on the expression control of CCL2. We previously demonstrated that inhibition of CCL2 expression is mediated by the nuclear corepressor 'Nuclear Receptor Corepressor 1' (NCoR1), which is recruited to a region 600 bp upstream of the transcriptional start site (TSS) in the promoter region of CCL2 (Pflüger-Müller et al., 2020). If NR4A mediated the NCoR1 recruitment, it should be shown that the receptor directly interacts with NCoR1 and recruits NR4A to the same site. Ideally, the interaction between NCoR1 and NR4A upon ligand binding should be demonstrated using co-immunoprecipitation. In particular, NCoR1, a 270 kDa protein, could not be immune-precipitated or overexpressed in HAoSMCs. As an alternative, the NanoBit reporter gene assay was performed, which is a luciferase-based bimolecular complementation assay to study protein–protein interaction in real time (Chumakov et al., 2012). As one part, NR4A was used ('Large BiT') and as second part, NCoR1 ('Small BiT'). Indeed, AEA but not the endocannabinoids PEA and OEA increased the luminescence signal in this assay, demonstrating that NR4A1 and NR4A2 interacted with the nuclear corepressor upon agonist stimulation (Figure 4a). To obtain direct proof of binding of NR4A to the CCL2 gene, chromatin immunoprecipitation (ChIP) experiments were performed. Indeed, AEA increased the abundance of NR4A1 and NR4A2 600 bp upstream of the CCL2 TSS indicating a direct interaction (Figure 4b). These findings were supported by a JASPAR motif analysis, which identified a binding site for both NR4A1 and NR4A2 in the same region (Figures 4c and S4). Collectively, these data demonstrated that AEA binds and activates NR4A1 and NR4A2 nuclear receptors. These receptors subsequently interact with their DNA binding elements and thereby facilitates recruitment of the corepressor NCoR1 to the promoter.

3.6 | Nuclear orphan receptor family NR4A mediate anandamide (AEA) signalling in SMCs

If NR4A receptors actually mediate the anti-inflammatory effect of AEA, depletion of the receptors would be expected to abolish this effect. SiRNA-mediated knockdown (Figures 5a and S1b–f) as well as CRISPR/Cas9-mediated knockout (Figures 5b and S1b) of NR4A1, NR4A2 and NR4A3 was established. These experiments demonstrated that loss of NR4A1 or NR4A2 expression, but not of NR4A3, blocked the anti-inflammatory effect of AEA (Figure 5a,b). These findings are in accordance with the thermophoresis data, in which AEA only bound NR4A1 and NR4A2. Collectively, these data demonstrate that in the present model the functional effects of AEA are mediated by NR4A1 and NR4A2.

3.7 | NR4A receptors mediate (AEA) responses in vivo

Although the present data strongly suggest that NR4A receptors and not CB receptors mediate the anti-inflammatory effect of AEA, it is a limitation that the experiments were carried out in cultured cells. During culture, de-differentiation of cells occurs, and expression or signalling of GPCRs, such as CB receptors, can be lost. To confirm that NR4A receptors are of importance for AEA signalling under more physiological conditions, confirmation of these data in native tissue was needed, ideally by knockout studies. Therefore, tamoxifen-inducible global NR4A1 and NR4A2 as well as NR4A1/A2 double knockout mice were generated by crossing NR4A1/2 floxed mice with CMV-CreERT2-deleter mice. Given the low half-life of AEA as well as its systemic effects upon application, specific models were sought to test the responses relevant here. As an experimental model closely resembling the cell culture conditions, short-term organ culture was conducted using aortae from these mice. Vessels were harvested and cut into 1 mm sized aortic rings, which were cultured overnight.

FIGURE 3 AEA interacts with the nuclear orphan receptor family NR4A. (a) CCL2 RT-qPCR of HAoSMC treated with cytosporone B (CsnB), 4-chlorophenyl-3,3′-diindolylmethane (CDIM-12) and prostaglandin A_1 (PGA1) and IL1β. n=3. As n<5 for these experiments, statistical analysis was not carried out, and results should be regarded as preliminary. (b) NanoTemper microscale thermophoresis analysis of ligand binding to labelled NR4A1, NR4A2 and NR4A3. Solvent control or potential ligands were added at the indicated concentrations, and ΔF was quantified by $F_{CTL}-F_{ligand}$ for each concentration. (c) Overlay of 2D [^{1}H,^{15}N]-TROSY HSQC NMR data of ^{15}N-labelled Nurr1/NR4A2 LBD in the presence of 0.8% EtOH-d6 vehicle (black) or 1 M equivalent of AEA (orange). Selected residues with the largest CSP and peak intensity changes are annotated. (d) Quantitative differential NMR chemical shift perturbation (CSP) and peak intensity analysis of 15 N-labelled Nurr1/NR4A2 LBD ± 1X AEA. Dotted lines denote the cut-off for residues displaying CSP or peak intensity changes > 2 s.d. from the mean. (e) Residues with NMR CSP and peak intensity changes > 2 s.d. from the mean are displayed on the crystal structure of AEA-bound Nurr1 LBD. AEA covalently bound to Cys566 is displayed as sticks (green). (f) Architecture and principle of Gal4-hybrid reporter gene assay: this study uses two plasmid constructs. The first is pFA-CMV-NR4A-LBD, a Gal4 chimaera receptor with Gal4 DNA binding (Gal4-DBD) and NR4A ligand binding domains (NR4A-LBD). Each NR4A construct has a separate plasmid. The second is pGL4.35luc2p/9x, a reporter gene construct with nine repeats of GAL4 UAS driving luciferase (luc2P) expression. The Gal4 chimaera receptor binds to the Gal4 response element on the reporter construct, and ligand binding activates the LBD, inducing coactivator recruitment which then drives reporter gene expression. (g) Relative activation of GAL4-Nurr1/NR4A2 LBD mutants by AEA. Respective mutants were co-transfected in HAoSMC and treated with AEA for 4 h. Luciferase activity was determined as described in Section 2. Where n ≥ 5, one-way ANOVA and Mann–Whitney test. *P < 0.05. rel., relative to.

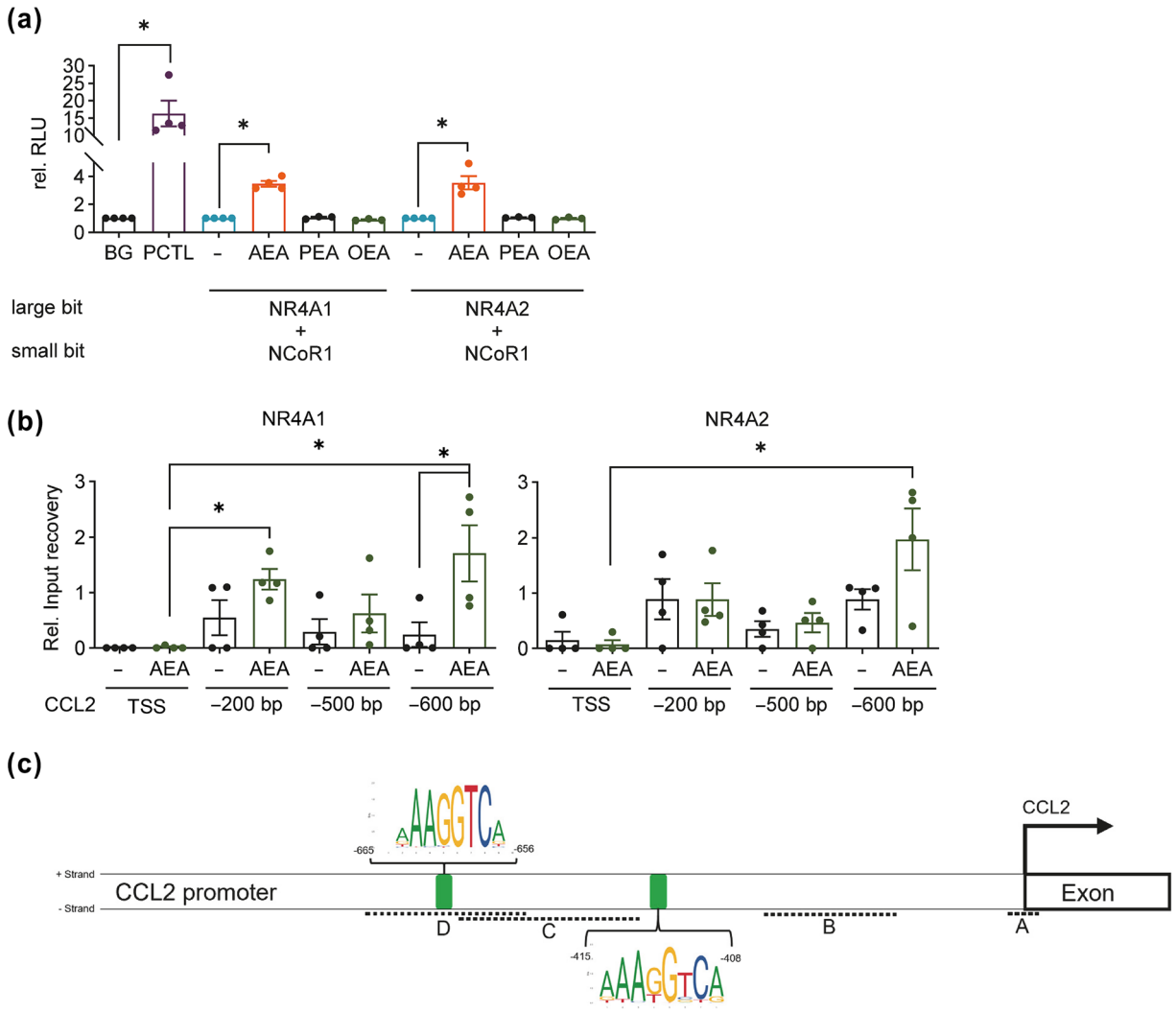

FIGURE 4 Nuclear receptor family NR4A1 and NR4A2 are recruited to the CCL2 gene locus upon AEA treatment. (a) HEK293 cells cotransfected with NR4A/NCoR1 or negative control (BG), as well as positive control (PCTL), followed by treatment with solvent or AEA (n = 4), PEA (n = 3) and OEA (n = 3) or rapamycin (30 μM) as a positive control in HT buffer. Interaction analysis using chemiluminescence measurement. As n < 5 for these experiments, statistical analysis was not carried out, and results should be regarded as preliminary. (b) ChIP of NR4A1 and NR4A2 at the CCL2 locus in HAoSMC treated with solvent or AEA. (c) CCL2 promotor region including NR4A1 and NR4A2 binding motif region and ChiP primer binding sites. Primer A refers to the region 'TSS', primer B to '−200 bp', primer C to '−500 bp' and primer D to '−600 bp' of the CCL2 promotor. rel., relative to.

Subsequently, AEA and IL1β stimulation was performed, and CCL2 expression was determined by RT-qPCR. IL1β induced a massive CCL2 increase in WT and NR4A2 KO mice, whereas the effect was smaller but still significant in NR4A1 and NR4A1/2 double KO mice (Figure 6). The latter effect was probably a consequence of NR4A1 already suppressing CCL2 under basal conditions, as knockout increased basal expression approximately fourfold (Figure S5). In agreement with our data in cultured HAoSMCs, AEA pretreatment of isolated mouse aortic segments attenuated IL1β-mediated CCL2-induction, although the inhibitory effect was smaller than in cultured cells. After knockout of NR4A1 and/or NR4A2, this effect was no longer significant (Figure 6). Collectively, these data demonstrate that also in the naïve vascular context, NR4A receptors mediate the response to AEA.

4 | DISCUSSION

In the present study, we identified AEA as an agonist for the orphan nuclear receptors NR4A1 and NR4A2, eliciting anti-inflammatory effects. We propose that the mode of action involves binding of the lipid to the ligand binding domain of the receptors, resulting in autoinduction followed by recruitment to gene promoters. At this site of action, the nuclear corepressor complex NCoR1 is recruited/retained, facilitating histone deacetylation, which causes attenuation of gene transcription (Pflüger-Müller et al., 2020).

Endocannabinoid levels are known to be altered during inflammation (Bátkai et al., 2007; Pacher & Steffens, 2009). It has been suggested that with increasing endocannabinoid levels in the plasma, inflammation decreases. This inverse correlation is also seen between

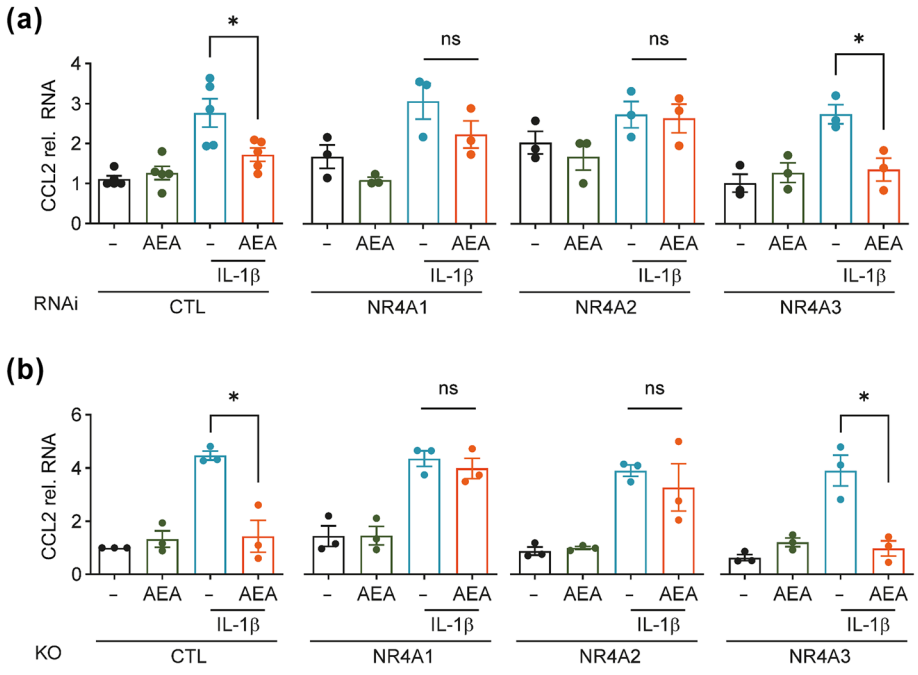

FIGURE 5 Nuclear orphan receptor family NR4A is essential for AEA signalling in vitro. (a) CCL2 RT-qPCR of HAoSMC after treatment with solvent or AEA and IL1β following siRNA-mediated knockdown of NR4A1 (n = 3), NR4A2 (n = 3) or NR4A3 (n = 3) (40 nM siRNA, 72 h). Where n ≥ 5, One-way ANOVA and Mann–Whitney test. *P < 0.05. (b) CCL2 RT-qPCR of HAoSMC transduced with lentiviral vectors for CRISPR/Cas9 and gRNAs targeting NR4A1 (n = 3), A2 (n = 3) or A3 (n = 3). Treatment with solvent or AEA and IL1β. As n < 5, statistical analysis was not carried out and results should be regarded as preliminary. rel., relative to.

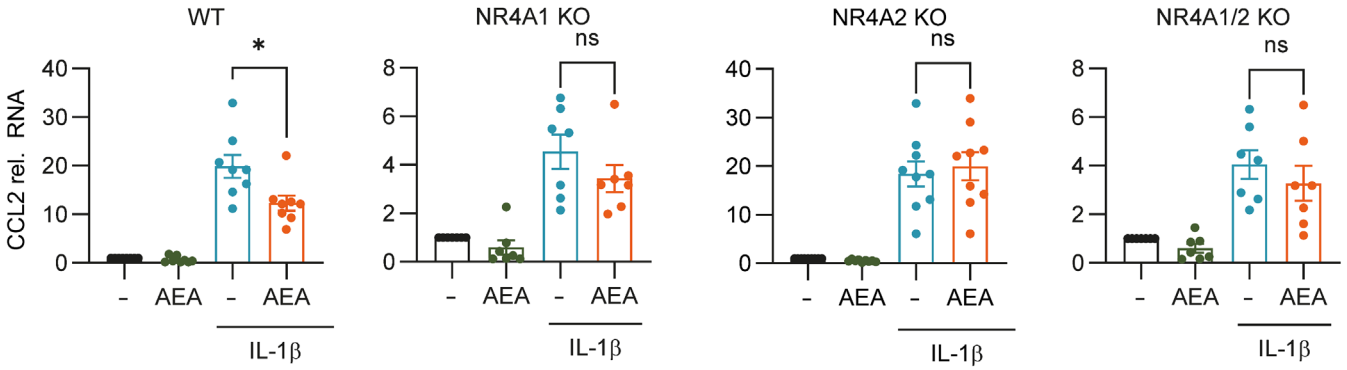

FIGURE 6 NR4A receptors mediate AEA responses in aortic rings. (a) CCL2 RT-qPCR of murine aortic rings from WT, NR4A1, NR4A2 or NR4A1/2 KO mice, treated with solvent or AEA and IL1β. n = 7, 1-way ANOVA. *P < 0.05. rel., relative to.

endocannabinoids and IL-6 or CCL2 levels (Gestrich et al., 2015). Our data support those findings, showing that the endocannabinoid AEA reduced the IL1β-induced CCL2 expression. Interestingly, only AEA, but not 2-AG, elicited this effect, arguing against an involvement of CB receptors. Indeed, the AEA-mediated effect on IL1β-induced gene expression was independent of the classical, so far known endocannabinoid receptors. Indeed, after exposure to PTX, which ADP-ribosylates Gi family proteins (Mangmool & Kurose, 2011), or knockout of CB_1/CB_2 receptors, responses to AEA remained unaffected, which rules out signalling via the classical endocannabinoid receptors. With the aid also of RNAi-mediated knock-down, the nuclear receptor family of PPARs could be excluded as AEA targets for the present anti-inflammatory actions. However, RNA-Seq revealed induction of another nuclear receptor family, namely, NR4As, which so far has not been linked to endocannabinoid signalling. In fact, this effect was most pronounced for NR4A1 and NR4A2. NR4A3, in contrast, was more strongly induced by IL1β.

Although not in the focus of endocannabinoid research, NR4A receptors have been studied for long as targets in inflammatory conditions (Rodríguez-Calvo et al., 2017). The NR4A family consists of three members, namely, Nur77 (NR4A1), Nurr-related factor (Nurr)1 (NR4A2) and neuron-derived orphan receptor (NOR)-1 (NR4A3) (Martínez-González & Badimon, 2005; Pols et al., 2007). In mice, NR4A1 deletion resulted in polarization of macrophages towards a pro-inflammatory M1 phenotype as well as amplifying atherosclerosis development (Hamers et al., 2013). Loss of NR4A2 in mice is associated with increased atherosclerosis by promoting smooth muscle cell proliferation and inflammation (Bonta et al., 2006). NR4A3 elicits an opposing function to NR4A1 and NR4A2, as NR4A3 promotes atherosclerosis in mice by enhancing the recruitment of monocytes to the vascular

wall (Zhao et al., 2010). Collectively, NR4A1 and NR4A2 appear to protect against atherosclerosis, whereas NR4A3 seems to be pro-atherosclerotic. This concept nicely aligns with our observation that AEA elicits an anti-inflammatory function through NR4A1 or NR4A2.

It was still interesting to note that to some extent both NR4A1 and NR4A2 were involved in AEA signalling. Potentially, this is the consequence of the fact that the receptors control gene expression as dimers. For both not only function in the monomeric form but also—and more importantly—as homodimer and heterodimer has been reported (Kurakula et al., 2014). Moreover, NR4A family members share a high degree of sequence similarity in their ligand-binding domains (LBDs) and DNA-binding domains (DBDs), yet they are highly diverse in their N-terminal domains, which include activation function 1 (AF1) (Pearen & Muscat, 2010). The transcriptional activity of the receptors is therefore activated by binding of a polyunsaturated fatty acid at the LBD, followed by recruitment of cofactors, which then determine whether the receptors act as gene repressor or activator (Bonta et al., 2010; Hamers et al., 2013; Kurakula et al., 2014).

As is common for nuclear receptors, NR4A receptors comprise distinct functional domains that include an N-terminal activation function 1 (AF-1) domain, a central DNA-binding domain with two zinc fingers and a C-terminal LBD (Rodríguez-Calvo et al., 2017). However, unlike other NRs, NR4A receptors inherit an atypical LBD as X-ray crystallography studies reveal that the LBD of NR4A2 contains hydrophobic residues occupying the space instead of the ligand-binding pocket found in other NRs (Wang et al., 2003). Similar, NR4A1 and NR4A3 exhibit unique hydrophilic surfaces in their LBDs (Wansa et al., 2002; Wansa et al., 2003). Hence, the NR4A receptor family has been originally classified as an orphan receptor family or even nuclear receptors without ligand binding site (Codina et al., 2004; Wang et al., 2003). Despite this, some poly-unsaturated fatty acids such as arachidonic acid or docosahexaenoic acid (DHA), but not saturated fatty acids, have been identified as ligands. NMR spectroscopy has identified direct binding of DHA to the canonical ligand binding pocket of NR4A2 (de Vera et al., 2016) and bind via an induced fit mechanism involving a conformational change after ligand binding (de Vera et al., 2019), which likely explains why we were unable to obtain a co-crystal structure of the AEA-bound NR4A2 LBD. Endocannabinoids themselves are derivatives of arachidonic acid and can therefore be classified as polyunsaturated fatty acids (McDougle et al., 2014). Hence, it was plausible that AEA can also act as receptor ligand, and it was rather surprising that the other endocannabinoids studied here did not activate NR4A.

5 | CONCLUSION

In the present study, we have presented evidence that AEA mediates anti-inflammatory effects in vascular smooth muscle cells via a mechanism that is independent of the classical, so far known endocannabinoid receptors. Instead, we identified AEA as a novel ligand of NR4A1 and NR4A2, which mediate the anti-inflammatory effects of this endocannabinoid. Based on these observations, our study paves the way for the development of novel NR4A agonists as novel anti-inflammatory agents.

AUTHOR CONTRIBUTIONS

T. Teichmann: Conceptualization (lead); data curation (lead); formal analysis (lead); investigation (lead); methodology (lead); validation (lead); visualization (lead); writing—original draft (lead). **B. Pflüger-Müller:** Conceptualization (lead); data curation (lead); formal analysis (lead); investigation (lead); methodology (lead); validation (lead); visualization (lead). **V. M. M. Giménez:** Data curation (supporting); formal analysis (supporting); investigation (supporting); methodology (supporting). **F. Sailer:** Data curation (supporting). **H. Dirks:** Data curation (supporting). **S. Zehr:** Formal analysis (supporting); visualization (supporting). **T. Warwick:** Formal analysis (supporting); visualization (supporting). **F. Brettner:** Data curation (supporting). **P. Munoz-Tello:** Data curation (supporting). **A. Zimmer:** Resources (supporting). **I. Tegeder:** Investigation (supporting); methodology (supporting). **D. Thomas:** Data curation (supporting). **R. Gurke:** Data curation (supporting); methodology (supporting). **S. Günther:** Data curation (supporting). **J. Heering:** Data curation (supporting); methodology (supporting). **E. Proschak:** Investigation (supporting); methodology (supporting). **G. Geisslinger:** Investigation (supporting); methodology (supporting). **I.-S. Bibli:** Investigation (supporting). **D. M. zu Heringdorf:** Investigation (supporting); methodology (supporting). **W. Manucha:** Funding acquisition (equal); investigation (supporting); methodology (supporting). **M. Windbergs:** Investigation (supporting). **S. Knapp:** Investigation (supporting); methodology (supporting). **A. Weigert:** Investigation (supporting). **M. S. Leisegang:** Conceptualization (lead); data curation (supporting); investigation (lead); methodology (lead). **D. Kojetin:** Funding acquisition (equal); investigation (equal); methodology (equal); visualization (equal). **R. P. Brandes:** Conceptualization (lead); funding acquisition (lead); project administration (lead); supervision (lead); validation (lead); visualization (lead); writing—original draft (lead).

ACKNOWLEDGEMENTS

The authors are grateful for the excellent technical assistance of Katalin Pálfi and Judit Ponce. Open Access funding enabled and organized by Projekt DEAL.

CONFLICT OF INTEREST STATEMENT

The authors declare no conflict of interest.

DATA AVAILABILITY STATEMENT

The data that support the findings of this study are openly available in at the public NCBI GEO database under the accession number GSE131732.

DECLARATION OF TRANSPARENCY AND SCIENTIFIC RIGOUR

This declaration acknowledges that this paper adheres to the principles for transparent reporting and scientific rigour of preclinical research as stated in the BJP guidelines for Natural Products Research, Design and Analysis, Immunoblotting and Immunochemistry

and Animal Experimentation and as recommended by funding agencies, publishers and other organizations engaged with supporting research.

ORCID

Tom Teichmann https://orcid.org/0009-0009-5402-3834
Irmgard Tegeder https://orcid.org/0000-0001-7524-8025

REFERENCES

Alexander, S. P. H., Christopoulos, A., Davenport, A. P., Kelly, E., Mathie, A. A., Peters, J. A., Veale, E. L., Armstrong, J. F., Faccenda, E., Harding, S. D., Davies, J. A., Abbracchio, M. P., Abraham, G., Agoulnik, A., Alexander, W., Al-Hosaini, K., Bäck, M., Baker, J. G., Barnes, N. M., … Ye, R. D. (2023). The Concise Guide to PHARMACOLOGY 2023/24: G protein-coupled receptors. *British Journal of Pharmacology*, *180*, S23–S144. https://doi.org/10.1111/bph.16177

Alexander, S. P. H., Cidlowski, J. A., Kelly, E., Mathie, A. A., Peters, J. A., Veale, E. L., Armstrong, J. F., Faccenda, E., Harding, S. D., Davies, J. A., Coons, L., Fuller, P. J., Korach, K. S., & Young, M. J. (2023). The Concise Guide to PHARMACOLOGY 2023/24: Nuclear hormone receptors. *British Journal of Pharmacology*, *180*(S2), S223–S240. https://doi.org/10.1111/bph.16179

Alexander, S. P. H., Fabbro, D., Kelly, E., Mathie, A. A., Peters, J. A., Veale, E. L., Armstrong, J. F., Faccenda, E., Harding, S. D., Davies, J. A., Annett, S., Boison, D., Burns, K. E., Dessauer, C., Gertsch, J., Helsby, N. A., Izzo, A. A., Ostrom, R., Papapetropoulos, A., … Wong, S. S. (2023). The concise guide to PHARMACOLOGY 2023/24: Enzymes. *British Journal of Pharmacology*, *180*, S289–S373. https://doi.org/10.1111/bph.16181

Alexander, S. P. H., Mathie, A. A., Peters, J. A., Veale, E. L., Striessnig, J., Kelly, E., Armstrong, J. F., Faccenda, E., Harding, S. D., Davies, J. A., Aldrich, R. W., Attali, B., Baggetta, A. M., Becirovic, E., Biel, M., Bill, R. M., Caceres, A. I., Catterall, W. A., Conner, A. C., … Zhu, M. (2023). The Concise Guide to PHARMACOLOGY 2023/24: Ion channels. *British Journal of Pharmacology*, *180*, S145–S222. https://doi.org/10.1111/bph.16178

Alexander, S. P. H., Roberts, R. E., Broughton, B. R. S., Sobey, C. G., George, C. H., Stanford, S. C., Cirino, G., Docherty, J. R., Giembycz, M. A., Hoyer, D., Insel, P. A., Izzo, A. A., Ji, Y., MacEwan, D. J., Mangum, J., Wonnacott, S., & Ahluwalia, A. (2018). Goals and practicalities of immunoblotting and immunohistochemistry: A guide for submission to the British Journal of Pharmacology. *British Journal of Pharmacology*, *175*, 407–411. https://doi.org/10.1111/bph.14112

Andrews, S. (2010). FastQC: A quality control tool for high throughput sequence data. http://www.bioinformatics.babraham.ac.uk/projects/fastqc

Baranowska-Kuczko, M., Kozłowska, H., Kozłowski, M., Schlicker, E., Kloza, M., Surażyński, A., Grzęda, E., & Malinowska, B. (2014). Mechanisms of endothelium-dependent relaxation evoked by anandamide in isolated human pulmonary arteries. *Naunyn-Schmiedeberg's Archives of Pharmacology*, *387*(5), 477–486. https://doi.org/10.1007/s00210-014-0961-9

Bátkai, S., Osei-Hyiaman, D., Pan, H., El-Assal, O., Rajesh, M., Mukhopadhyay, P., Hong, F., Harvey-White, J., Jafri, A., Haskó, G., Huffman, J. W., Gao, B., Kunos, G., & Pacher, P. (2007). Cannabinoid-2 receptor mediates protection against hepatic ischemia/reperfusion injury. *FASEB Journal : Official Publication of the Federation of American Societies for Experimental Biology*, *21*(8), 1788–1800. https://doi.org/10.1096/fj.06-7451com

Battista, N., di Tommaso, M., Bari, M., & Maccarrone, M. (2012). The endocannabinoid system: An overview. *Frontiers in Behavioral Neuroscience*, *6*, 9. https://doi.org/10.3389/fnbeh.2012.00009

Beltramo, M., Stella, N., Calignano, A., Lin, S. Y., Makriyannis, A., & Piomelli, D. (1997). Functional role of high-affinity anandamide transport, as revealed by selective inhibition. *Science (New York, N.Y.)*, *277*(5329), 1094–1097. https://doi.org/10.1126/science.277.5329.1094

Bibli, S.-I., Hu, J., Sigala, F., Wittig, I., Heidler, J., Zukunft, S., Tsilimigras, D. I., Randriamboavonjy, V., Wittig, J., Kojonazarov, B., Schürmann, C., Siragusa, M., Siuda, D., Luck, B., Abdel Malik, R., Filis, K. A., Zografos, G., Chen, C., Wang, D. W., … Fleming, I. (2019). Cystathionine γ Lyase sulfhydrates the RNA binding protein human antigen R to preserve endothelial cell function and delay Atherogenesis. *Circulation*, *139*(1), 101–114. https://doi.org/10.1161/CIRCULATIONAHA.118.034757

Bonta, P. I., Pols, T. W. H., van Tiel, C. M., Vos, M., Arkenbout, E. K., Rohlena, J., Koch, K. T., de Maat, M. P. M., Tanck, M. W. T., de Winter, R. J., Pannekoek, H., Biessen, E. A. L., Bot, I., & de Vries, C. J. M. (2010). Nuclear receptor Nurr1 is expressed in and is associated with human restenosis and inhibits vascular lesion formation in mice involving inhibition of smooth muscle cell proliferation and inflammation. *Circulation*, *121*(18), 2023–2032. https://doi.org/10.1161/CIRCULATIONAHA.109.885673

Bonta, P. I., van Tiel, C. M., Vos, M., Pols, T. W. H., van Thienen, J. V., Ferreira, V., Arkenbout, E. K., Seppen, J., Spek, C. A., van der Poll, T., Pannekoek, H., & de Vries, C. J. M. (2006). Nuclear receptors Nur77, Nurr1, and NOR-1 expressed in atherosclerotic lesion macrophages reduce lipid loading and inflammatory responses. *Arteriosclerosis, Thrombosis, and Vascular Biology*, *26*(10), 2288–2294. https://doi.org/10.1161/01.ATV.0000238346.84458.5d

Chumakov, S. P., Kravchenko, Y. E., & Chumakov, P. M. (2012). Protein complementation as tool for studying protein-protein interactions in living cells. *Molecular Biology*, *46*(5), 627–638. https://doi.org/10.1134/S0026893312050020

Codina, A., Benoit, G., Gooch, J. T., Neuhaus, D., Perlmann, T., & Schwabe, J. W. R. (2004). Identification of a novel co-regulator interaction surface on the ligand binding domain of Nurr1 using NMR footprinting. *The Journal of Biological Chemistry*, *279*(51), 53338–53345. https://doi.org/10.1074/jbc.M409096200

Curtis, M. J., Alexander, S. P. H., Cirino, G., George, C. H., Kendall, D. A., Insel, P. A., Izzo, A. A., Ji, Y., Panettieri, R. A., Patel, H. H., Sobey, C. G., Stanford, S. C., Stanley, P., Stefanska, B., Stephens, G. J., Teixeira, M. M., Vergnolle, N., & Ahluwalia, A. (2022). Planning experiments: Updated guidance on experimental design and analysis and their reporting III. *British Journal of Pharmacology*, *179*(15), 3907–3913. https://doi.org/10.1111/bph.15868

Davis, M. P. A., van Dongen, S., Abreu-Goodger, C., Bartonicek, N., & Enright, A. J. (2013). Kraken: A set of tools for quality control and analysis of high-throughput sequence data. *Methods (San Diego, Calif.)*, *63*(1), 41–49. https://doi.org/10.1016/j.ymeth.2013.06.027

de Vera, I. M. S., Giri, P. K., Pankaj, K., Munoz-Tello, P., Brust, R., Fuhrmann, J., Matta-Camacho, E., Shang, J., Campbell, S., Wilson, H. D., Granados, J., Gardner, W. J., Creamer, T. P., Solt, L. A., & Kojetin, D. J. (2016). Identification of a binding site for unsaturated fatty acids in the orphan nuclear receptor Nurr1. *ACS Chemical Biology*, *11*(7), 1795–1799. https://doi.org/10.1021/acschembio.6b00037

de Vera, I. M. S., Munoz-Tello, P., Zheng, J., Dharmarajan, V., Marciano, D. P., Matta-Camacho, E., Giri, P., Kumar, K. P., Shang, J., Hughes, T. S., Rance, M., Griffin, P. R., & Kojetin, D. J. (2019). Defining a canonical ligand-binding pocket in the orphan nuclear receptor Nurr1. *Structure (London, England: 1993)*, *27*(1), 66–77.e5. https://doi.org/10.1016/j.str.2018.10.002

Dobin, A., Davis, C. A., Schlesinger, F., Drenkow, J., Zaleski, C., Jha, S., Batut, P., Chaisson, M., & Gingeras, T. R. (2013). Star: Ultrafast universal RNA-seq aligner. *Bioinformatics (Oxford, England)*, *29*(1), 15–21. https://doi.org/10.1093/bioinformatics/bts635

Ellis, E. F., Moore, S. F., & Willoughby, K. A. (1995). Anandamide and delta 9-THC dilation of cerebral arterioles is blocked by indomethacin. *The American Journal of Physiology*, *269*(6 Pt 2), H1859–H1864. https://doi.org/10.1152/ajpheart.1995.269.6.H1859

Elron-Gross, I., Glucksam, Y., Melikhov, D., & Margalit, R. (2008). Cyclooxygenase inhibition by diclofenac formulated in bioadhesive carriers. *Biochimica et Biophysica Acta*, *1778*(4), 931–936. https://doi.org/10.1016/j.bbamem.2008.01.002

Fornes, O., Castro-Mondragon, J. A., Khan, A., van der Lee, R., Zhang, X., Richmond, P. A., Modi, B. P., Correard, S., Gheorghe, M., Baranašić, D., Santana-Garcia, W., Tan, G., Chèneby, J., Ballester, B., Parcy, F., Sandelin, A., Lenhard, B., Wasserman, W. W., & Mathelier, A. (2020). Jaspar 2020: Update of the open-access database of transcription factor binding profiles. *Nucleic Acids Research*, *48*(D1), D87–D92. https://doi.org/10.1093/nar/gkz1001

Gestrich, C., Duerr, G. D., Heinemann, J. C., Meertz, A., Probst, C., Roell, W., Schiller, W., Zimmer, A., Bindila, L., Lutz, B., Welz, A., & Dewald, O. (2015). Activation of endocannabinoid system is associated with persistent inflammation in human aortic aneurysm. *BioMed Research International*, *2015*, 456582. https://doi.org/10.1155/2015/456582

Grill, M., Högenauer, C., Blesl, A., Haybaeck, J., Golob-Schwarzl, N., Ferreirós, N., Thomas, D., Gurke, R., Trötzmüller, M., Köfeler, H. C., Gallé, B., & Schicho, R. (2019). Members of the endocannabinoid system are distinctly regulated in inflammatory bowel disease and colorectal cancer. *Scientific Reports*, *9*(1), 2358. https://doi.org/10.1038/s41598-019-38865-4

Hamers, A. A. J., Hanna, R. N., Nowyhed, H., Hedrick, C. C., & de Vries, C. J. M. (2013). Nr4a nuclear receptors in immunity and atherosclerosis. *Current Opinion in Lipidology*, *24*(5), 381–385. https://doi.org/10.1097/MOL.0b013e3283643eac

Hammond, S. L., Safe, S., & Tjalkens, R. B. (2015). A novel synthetic activator of Nurr1 induces dopaminergic gene expression and protects against 6-hydroxydopamine neurotoxicity in vitro. *Neuroscience Letters*, *607*, 83–89. https://doi.org/10.1016/j.neulet.2015.09.015

Jerabek-Willemsen, M., André, T., Wanner, R., Roth, H. M., Duhr, S., Baaske, P., & Breitsprecher, D. (2014). MicroScale thermophoresis: Interaction analysis and beyond. *Journal of Molecular Structure*, *1077*, 101–113. https://doi.org/10.1016/j.molstruc.2014.03.009

Johnson, B. A. (2018). From raw data to protein backbone chemical shifts using NMRFx processing and NMRViewJ analysis. *Methods in Molecular Biology (Clifton, N.J.)*, *1688*, 257–310. https://doi.org/10.1007/978-1-4939-7386-6_13

Kagaya, S., Ohkura, N., Tsukada, T., Miyagawa, M., Sugita, Y., Tsujimoto, G., Matsumoto, K., Saito, H., & Hashida, R. (2005). Prostaglandin A2 acts as a transactivator for NOR1 (NR4A3) within the nuclear receptor superfamily. *Biological & Pharmaceutical Bulletin*, *28*(9), 1603–1607. https://doi.org/10.1248/bpb.28.1603

Kurakula, K., Koenis, D. S., van Tiel, C. M., & de Vries, C. J. M. (2014). Nr4a nuclear receptors are orphans but not lonesome. *Biochimica et Biophysica Acta*, *1843*(11), 2543–2555. https://doi.org/10.1016/j.bbamcr.2014.06.010

Liao, Y., Smyth, G. K., & Shi, W. (2014). Featurecounts: An efficient general purpose program for assigning sequence reads to genomic features. *Bioinformatics (Oxford, England)*, *30*(7), 923–930. https://doi.org/10.1093/bioinformatics/btt656

Ligresti, A., de Petrocellis, L., & di Marzo, V. (2016). From Phytocannabinoids to cannabinoid receptors and endocannabinoids: Pleiotropic physiological and pathological roles through complex pharmacology. *Physiological Reviews*, *96*(4), 1593–1659. https://doi.org/10.1152/physrev.00002.2016

Lilley, E., Stanford, S. C., Kendall, D. E., Alexander, S. P. H., Cirino, G., Docherty, J. R., George, C. H., Insel, P. A., Izzo, A. A., Ji, Y., Panettieri, R. A., Sobey, C. G., Stefanska, B., Stephens, G., Teixeira, M., & Ahluwalia, A. (2020). ARRIVE 2.0 and the *British Journal of Pharmacology*: Updated guidance for 2020. *British Journal of Pharmacology*, *177*, 3611–3616. https://doi.org/10.1111/bph.15178

Love, M. I., Huber, W., & Anders, S. (2014). Moderated estimation of fold change and dispersion for RNA-seq data with DESeq2. *Genome Biology*, *15*(12), 550. https://doi.org/10.1186/s13059-014-0550-8

Lu, H.-C., & Mackie, K. (2016). An introduction to the endogenous cannabinoid system. *Biological Psychiatry*, *79*(7), 516–525. https://doi.org/10.1016/j.biopsych.2015.07.028

Maccarrone, M. (2017). Metabolism of the endocannabinoid anandamide: Open questions after 25 years. *Frontiers in Molecular Neuroscience*, *10*, 166. https://doi.org/10.3389/fnmol.2017.00166

Mallet, C., Barrière, D. A., Ermund, A., Jönsson, B. A. G., Eschalier, A., Zygmunt, P. M., & Högestätt, E. D. (2010). Trpv1 in brain is involved in acetaminophen-induced antinociception. *PLoS ONE*, *5*(9), e12748. https://doi.org/10.1371/journal.pone.0012748

Mangmool, S., & Kurose, H. (2011). G(i/o) protein-dependent and -independent actions of pertussis toxin (PTX). *Toxins*, *3*(7), 884–899. https://doi.org/10.3390/toxins3070884

Martínez-González, J., & Badimon, L. (2005). The NR4A subfamily of nuclear receptors: New early genes regulated by growth factors in vascular cells. *Cardiovascular Research*, *65*(3), 609–618. https://doi.org/10.1016/j.cardiores.2004.10.002

McDougle, D. R., Kambalyal, A., Meling, D. D., & Das, A. (2014). Endocannabinoids anandamide and 2-arachidonoylglycerol are substrates for human CYP2J2 epoxygenase. *The Journal of Pharmacology and Experimental Therapeutics*, *351*(3), 616–627. https://doi.org/10.1124/jpet.114.216598

Michiels, P., Atkins, K., Ludwig, C., Whittaker, S., van Dongen, M., & Günther, U. (2010). Assignment of the orphan nuclear receptor Nurr1 by NMR. *Biomolecular NMR Assignments*, *4*(1), 101–105. https://doi.org/10.1007/s12104-010-9210-4

Munoz-Tello, P., Lin, H., Khan, P., de Vera, I. M. S., Kamenecka, T. M., & Kojetin, D. J. (2020). Assessment of NR4A ligands that directly bind and modulate the orphan nuclear receptor Nurr1. *Journal of Medicinal Chemistry*, *63*(24), 15639–15654. https://doi.org/10.1021/acs.jmedchem.0c00894

Munro, S., Thomas, K. L., & Abu-Shaar, M. (1993). Molecular characterization of a peripheral receptor for cannabinoids. *Nature*, *365*(6441), 61–65. https://doi.org/10.1038/365061a0

Norris, M., Fetler, B., Marchant, J., & Johnson, B. A. (2016). Nmrfx processor: A cross-platform NMR data processing program. *Journal of Biomolecular NMR*, *65*(3–4), 205–216. https://doi.org/10.1007/s10858-016-0049-6

Olivares, A. M., Moreno-Ramos, O. A., & Haider, N. B. (2015). Role of nuclear receptors in central nervous system development and associated diseases. *Journal of Experimental Neuroscience*, *9*(Suppl 2), 93–121. https://doi.org/10.4137/JEN.S25480

O'Sullivan, S. E. (2007). Cannabinoids go nuclear: Evidence for activation of peroxisome proliferator-activated receptors. *British Journal of Pharmacology*, *152*(5), 576–582. https://doi.org/10.1038/sj.bjp.0707423

Pacher, P., & Steffens, S. (2009). The emerging role of the endocannabinoid system in cardiovascular disease. *Seminars in Immunopathology*, *31*(1), 63–77. https://doi.org/10.1007/s00281-009-0145-8

Paguio, A., Stecha, P., Wood, K. V., & Fan, F. (2010). Improved dual-luciferase reporter assays for nuclear receptors. *Current Chemical Genomics*, *4*, 43–49. https://doi.org/10.2174/1875397301004010043

Pandey, R., Mousawy, K., Nagarkatti, M., & Nagarkatti, P. (2009). Endocannabinoids and immune regulation. *Pharmacological Research*, *60*(2), 85–92. https://doi.org/10.1016/j.phrs.2009.03.019

Pearen, M. A., & Muscat, G. E. O. (2010). Minireview: Nuclear hormone receptor 4A signaling: Implications for metabolic disease. *Molecular Endocrinology (Baltimore, Md.)*, *24*(10), 1891–1903. https://doi.org/10.1210/me.2010-0015

Pei, L., Castrillo, A., Chen, M., Hoffmann, A., & Tontonoz, P. (2005). Induction of NR4A orphan nuclear receptor expression in macrophages in response to inflammatory stimuli. *The Journal of Biological Chemistry*, *280*(32), 29256–29262. https://doi.org/10.1074/jbc.M502606200

Percie du Sert, N., Hurst, V., Ahluwalia, A., Alam, S., Avey, M. T., Baker, M., Browne, W. J., Clark, A., Cuthill, I. C., Dirnagl, U., Emerson, M., Garner, P., Holgate, S. T., Howells, D. W., Karp, N. A., Lazic, S. E., Lidster, K., MacCallum, C. J., Macleod, M., … Würbel, H. (2020). The ARRIVE guidelines 2.0: Updated guidelines for reporting animal research. *PLoS Biology*, *18*(7), e3000410. https://doi.org/10.1371/journal.pbio.3000410

Pertwee, R. G., Howlett, A. C., Abood, M. E., Alexander, S. P. H., di Marzo, V., Elphick, M. R., Greasley, P. J., Hansen, H. S., Kunos, G., Mackie, K., Mechoulam, R., & Ross, R. A. (2010). International Union of Basic and Clinical Pharmacology. Lxxix. Cannabinoid receptors and their ligands: Beyond CB_1 and CB_2. *Pharmacological Reviews*, *62*(4), 588–631. https://doi.org/10.1124/pr.110.003004

Pflüger-Müller, B., Oo, J. A., Heering, J., Warwick, T., Proschak, E., Günther, S., Looso, M., Rezende, F., Fork, C., Geisslinger, G., Thomas, D., Gurke, R., Steinhilber, D., Schulz, M., Leisegang, M. S., & Brandes, R. P. (2020). The endocannabinoid anandamide has an anti-inflammatory effect on CCL2 expression in vascular smooth muscle cells. *Basic Research in Cardiology*, *115*(3), 34. https://doi.org/10.1007/s00395-020-0793-3

Piscitelli, F., & di Marzo, V. (2012). "Redundancy" of endocannabinoid inactivation: New challenges and opportunities for pain control. *ACS Chemical Neuroscience*, *3*(5), 356–363. https://doi.org/10.1021/cn300015x

Pols, T. W. H., Bonta, P. I., & de Vries, C. J. M. (2007). Nr4a nuclear orphan receptors: Protective in vascular disease? *Current Opinion in Lipidology*, *18*(5), 515–520. https://doi.org/10.1097/MOL.0b013e3282ef77d1

Rajan, S., Jang, Y., Kim, C.-H., Kim, W., Toh, H. T., Jeon, J., Song, B., Serra, A., Lescar, J., Yoo, J. Y., Beldar, S., Ye, H., Kang, C., Liu, X.-W., Feitosa, M., Kim, Y., Hwang, D., Goh, G., Lim, K.-L., … Kim, K.-S. (2020). Pge1 and PGA1 bind to Nurr1 and activate its transcriptional function. *Nature Chemical Biology*, *16*(8), 876–886. https://doi.org/10.1038/s41589-020-0553-6

Rodríguez-Calvo, R., Tajes, M., & Vázquez-Carrera, M. (2017). The NR4A subfamily of nuclear receptors: Potential new therapeutic targets for the treatment of inflammatory diseases. *Expert Opinion on Therapeutic Targets*, *21*(3), 291–304. https://doi.org/10.1080/14728222.2017.1279146

Sanjana, N. E., Shalem, O., & Zhang, F. (2014). Improved vectors and genome-wide libraries for CRISPR screening. *Nature Methods*, *11*(8), 783–784. https://doi.org/10.1038/nmeth.3047

Schindelin, J., Arganda-Carreras, I., Frise, E., Kaynig, V., Longair, M., Pietzsch, T., Preibisch, S., Rueden, C., Saalfeld, S., Schmid, B., Tinevez, J.-Y., White, D. J., Hartenstein, V., Eliceiri, K., Tomancak, P., & Cardona, A. (2012). Fiji: An open-source platform for biological-image analysis. *Nature Methods*, *9*(7), 676–682. https://doi.org/10.1038/nmeth.2019

Sekiya, T., Kashiwagi, I., Inoue, N., Morita, R., Hori, S., Waldmann, H., Rudensky, A. Y., Ichinose, H., Metzger, D., Chambon, P., & Yoshimura, A. (2011). The nuclear orphan receptor Nr4a2 induces Foxp3 and regulates differentiation of CD4+ T cells. *Nature Communications*, *2*, 269. https://doi.org/10.1038/ncomms1272

Stanley, C. P., Hind, W. H., Tufarelli, C., O'Sullivan, S. E., & Saoirse, E. (2016). The endocannabinoid anandamide causes endothelium-dependent vasorelaxation in human mesenteric arteries. *Pharmacological Research*, *113*(Pt A), 356–363. https://doi.org/10.1016/j.phrs.2016.08.028

Tuma, R. F., & Steffens, S. (2012). Targeting the endocannabinod system to limit myocardial and cerebral ischemic and reperfusion injury. *Current Pharmaceutical Biotechnology*, *13*(1), 46–58. https://doi.org/10.2174/138920112798868665

Wang, Z., Benoit, G., Liu, J., Prasad, S., Aarnisalo, P., Liu, X., Xu, H., Walker, N. P. C., & Perlmann, T. (2003). Structure and function of Nurr1 identifies a class of ligand-independent nuclear receptors. *Nature*, *423*(6939), 555–560. https://doi.org/10.1038/nature01645

Wansa, K. D. S. A., Harris, J. M., & Muscat, G. E. O. (2002). The activation function-1 domain of Nur77/NR4A1 mediates trans-activation, cell specificity, and coactivator recruitment. *The Journal of Biological Chemistry*, *277*(36), 33001–33011. https://doi.org/10.1074/jbc.M203572200

Wansa, K. D. S. A., Harris, J. M., Yan, G., Ordentlich, P., & Muscat, G. E. O. (2003). The AF-1 domain of the orphan nuclear receptor NOR-1 mediates trans-activation, coactivator recruitment, and activation by the purine anti-metabolite 6-mercaptopurine. *The Journal of Biological Chemistry*, *278*(27), 24776–24790. https://doi.org/10.1074/jbc.M300088200

Willems, S., Kilu, W., Ni, X., Chaikuad, A., Knapp, S., Heering, J., & Merk, D. (2020). The orphan nuclear receptor Nurr1 is responsive to non-steroidal anti-inflammatory drugs. *Communications Chemistry*, *3*(1), 85. https://doi.org/10.1038/s42004-020-0331-0

Williamson, M. P. (2013). Using chemical shift perturbation to characterise ligand binding. *Progress in Nuclear Magnetic Resonance Spectroscopy*, *73*, 1–16. https://doi.org/10.1016/j.pnmrs.2013.02.001

Zhan, Y., Du, X., Chen, H., Liu, J., Zhao, B., Huang, D., Li, G., Xu, Q., Zhang, M., Weimer, B. C., Chen, D., Cheng, Z., Zhang, L., Li, Q., Li, S., Zheng, Z., Song, S., Huang, Y., Ye, Z., … Wu, Q. (2008). Cytosporone B is an agonist for nuclear orphan receptor Nur77. *Nature Chemical Biology*, *4*(9), 548–556. https://doi.org/10.1038/nchembio.106

Zhao, Y., & Bruemmer, D. (2010). Nr4a orphan nuclear receptors: Transcriptional regulators of gene expression in metabolism and vascular biology. *Arteriosclerosis, Thrombosis, and Vascular Biology*, *30*(8), 1535–1541. https://doi.org/10.1161/ATVBAHA.109.191163

Zhao, Y., Howatt, D. A., Gizard, F., Nomiyama, T., Findeisen, H. M., Heywood, E. B., Jones, K. L., Conneely, O. M., Daugherty, A., & Bruemmer, D. (2010). Deficiency of the NR4A orphan nuclear receptor NOR1 decreases monocyte adhesion and atherosclerosis. *Circulation Research*, *107*(4), 501–511. https://doi.org/10.1161/CIRCRESAHA.110.222083

Zimmer, A., Zimmer, A. M., Hohmann, A. G., Herkenham, M., & Bonner, T. I. (1999). Increased mortality, hypoactivity, and hypoalgesia in cannabinoid CB1 receptor knockout mice. *Proceedings of the National Academy of Sciences of the United States of America*, *96*(10), 5780–5785. https://doi.org/10.1073/pnas.96.10.5780

Zygmunt, P. M., Petersson, J., Andersson, D. A., Chuang, H., Sørgård, M., di Marzo, V., Julius, D., & Högestätt, E. D. (1999). Vanilloid receptors on sensory nerves mediate the vasodilator action of anandamide. *Nature*, *400*(6743), 452–457. https://doi.org/10.1038/22761

SUPPORTING INFORMATION

Additional supporting information can be found online in the Supporting Information section at the end of this article.

How to cite this article: Teichmann, T., Pflüger-Müller, B., Giménez, V. M. M., Sailer, F., Dirks, H., Zehr, S., Warwick, T., Brettner, F., Munoz-Tello, P., Zimmer, A., Tegeder, I., Thomas, D., Gurke, R., Günther, S., Heering, J., Proschak, E., Geisslinger, G., Bibli, I.-S., Heringdorf, D. M. z., … Brandes, R. P. (2024). The endocannabinoid anandamide mediates anti-inflammatory effects through activation of NR4A nuclear receptors. *British Journal of Pharmacology*, 1–19. https://doi.org/10.1111/bph.17366